IEEE Access
Multidisciplinary | Rapid Review | Open Access Journal

Received September 17, 2021, accepted October 20, 2021, date of publication October 22, 2021, date of current version November 1, 2021.

Digital Object Identifier 10.1109/ACCESS.2021.3122288

Polarization Aberration of a Non-Rotationally Symmetric Optical System With Freeform Surfaces

YILAN ZHANG[1], HAODONG SHI[2], AND HUILIN JIANG[2]

[1]College of Optoelectronic Engineering, Changchun University of Science and Technology, Changchun 130022, China
[2]State Key Laboratory of Applied Optics, National and Local Joint Engineering Research Center for Space Optoelectronics Technology, Changchun University of Science and Technology, Changchun 130022, China

Corresponding authors: Huilin Jiang (cclgdxkjs@163.com) and Haodong Shi (shihaodong08@163.com)

This work was supported in part by the National Natural Science Foundation of China under Grant 61805027 and Grant 61805028, and in part by the Scientific Research Foundation of the Education Department of Jilin Province, China, under Grant JJKH20190577KJ.

ABSTRACT Owing to the wide application of freeform surfaces in off-axis optical systems with large apertures, large fields of view, and long focus distances, the polarization effects caused by non-rotationally symmetrical surfaces have a significant impact on the system's polarization imaging quality and measurement accuracy. In this study, considering the problem of the aforementioned polarization effects, a polarization aberration analysis method based on the Jones notation using the fringe Zernike polynomials freeform surface is proposed. A full-field polarization aberration analysis model of a non-rotationally symmetric reflection optical system with a freeform surface is constructed. The effect of freeform surfaces on the distribution characteristics of the proposed model is demonstrated. Through the full-field polarization ray tracing of the field-of-view off-axis optical system, three kinds of polarization aberrations, comprising phase aberration, retardance, and diattenuation are obtained, after the introduction of the Zernike polynomial freeform surface. Finally, a full-field polarization aberration analysis is carried out for a wide-field off-axis three-reflection optical system with freeform surfaces. The results show that the phase aberration of a non-rotationally symmetric optical system with freeform surfaces is directly related to the freeform surface shape. The full-field of view distribution of the retardance and diattenuation caused by the free-form surface is 52.5% of the overall retardance and diattenuation distribution of the system. The proposed method will be of great significance for improving the accuracy of systems in deep-space telescopes and lithography objectives.

INDEX TERMS Jones matrix, freeform surface, polarization ray tracing, polarization aberration, non-rotationally symmetric system.

I. INTRODUCTION

Polarization aberration represents the change in the polarization state of light passing through an optical system. One of the main factors causing polarization aberration is the non-perpendicular ray incident on the optical interface. Although non-rotationally symmetric optical systems with freeform can effectively solve the bottleneck of traditional coaxial optical systems that have difficulty achieving a large aperture, large field of view, and long focal length at the same time, these non-rotationally symmetric optical systems also introduce polarization aberration. For high-precision optical systems such as large relative aperture lithography lenses and ultra-long focal length astronomical telescopes, the impact of polarization aberration on the imaging quality and measurement accuracy of the system cannot be neglected [1]. Therefore, it is helpful to analyze and control the polarization aberration distribution of the optical system to understand the mechanism of the polarization aberration of the freeform surface on the non-rotationally symmetric optical system. This would facilitate satisfying the high-precision imaging requirements of special optical systems.

In 1987, Chipman proposed the theory of polarization aberration and decomposed diattenuation and retardance using the eigenvalues of the Jones matrix [2]. James P decomposed and expanded the polarization aberration function into a

The associate editor coordinating the review of this manuscript and approving it for publication was Pallab K. Choudhury.

polarization aberration matrix. He also analyzed the polarization aberration of rotationally symmetric systems [3]. Sasian explained polarization aberration from the perspective of field and wavefront surfaces [4]. James *et al.* analyzed the effect of polarization aberration on the imaging quality of astronomical telescope systems [1]. Hui Wang et al. studied miniaturized low profile and second-order multi-band polarization selective surface [5]. Zhenyang Ding demonstrated the compact in situ mueller-matrix polarimetry based on binary polarization rotators [6]. Xiangru studied an orthogonal polynomial that can describe the polarization aberration of a rotationally symmetric system [7]. It can show the relationship between the polarization aberration, pupil, and field of view. At present, there is no theoretical model or standard method for the analysis of the polarization aberration characteristics of non-rotationally symmetric optical systems with freeform. It is difficult for designers to predict the impact of polarization aberrations on the imaging quality of such optical systems. The designers can only use optical design software to trace the polarized ray of the optical system after the design is completed, which greatly reduces the design efficiency and applicability of polarization imaging systems. Therefore, the study of polarization aberration distribution characteristics of non-rotationally symmetric optical systems with freeform can not only further perfect the theoretical system of polarization aberration, but also provide important guidance for the application of freeform surfaces in non-rotationally symmetric polarization imaging systems.

In Section 2, we introduce the basic theory of non-rotationally symmetric system polarization aberration and construct an analytical model for non-rotationally symmetric system polarization aberration of freeform surfaces with fringe Zernike polynomials as the characterizing function. In Section 3, through a single-mirror system with a freeform surface, the influence of the freeform surface shape on the polarization aberration distribution of the non-rotationally symmetric optical system, such as phase aberration, diattenuation, and retardance, is analyzed. This theory was verified. In Section 4, a non-rotationally symmetric optical system with freeform surfaces is designed, and its polarization characteristics are analyzed. Appendix A derives the polarization transmission matrix of the freeform surface optical system.

II. POLARIZATION ABERRATION ANALYSIS METHOD OF FREEFORM SURFACE OPTICAL SYSTEM

A. JONES MATRICES

This section focuses on the relative changes in the phase and amplitude of polarized light in optical systems. Compared with the Muller matrix, the Jones representation can more intuitively express the relationship between phase aberration, diattenuation, retardance, and freeform surfaces. Therefore, the polarization theory based on the Jones vector and Jones matrix is employed in this study [8].

The Jones matrix $\boldsymbol{J} = \begin{bmatrix} J_{11} & J_{12} \\ J_{21} & J_{22} \end{bmatrix}$ is a complex matrix of 2×2, which can be represented by the identity matrix $\boldsymbol{\sigma_0}$ and Pauli matrix $\boldsymbol{\sigma}_k$ $(k = 1, 2, 3)$ [8]:

$$\boldsymbol{\sigma_0} = \begin{pmatrix} 1 & 0 \\ 0 & 1 \end{pmatrix}, \quad \boldsymbol{\sigma_1} = \begin{pmatrix} 1 & 0 \\ 0 & -1 \end{pmatrix}, \boldsymbol{\sigma_2} = \begin{pmatrix} 0 & 1 \\ 1 & 0 \end{pmatrix}, \boldsymbol{\sigma_3} = \begin{pmatrix} 0 & -i \\ i & 0 \end{pmatrix}, \tag{1}$$

$$\begin{aligned} \boldsymbol{J} &= \exp\left(c_0\boldsymbol{\sigma_0} + c_1\boldsymbol{\sigma_1} + c_2\boldsymbol{\sigma_2} + c_3\boldsymbol{\sigma_3}\right) \\ &= \exp\left[(\rho_0 + i\phi_0)\,\boldsymbol{\sigma_0} + (\rho_1 + i\phi_1)\,\boldsymbol{\sigma_1} + (\rho_2 + i\phi_2)\,\boldsymbol{\sigma_2} \right. \\ &\quad \left. + (\rho_3 + i\phi_3)\,\boldsymbol{\sigma_3}\right], \end{aligned} \tag{2}$$

where c_k is the coefficient of $\boldsymbol{\sigma_k}$, and ρ_k and ϕ_k are real numbers. A Jones matrix is typically used to describe the entire beam cross-section through the optical element. The polarization change of the optical system along different optical paths can be represented as a polarization aberration function $\boldsymbol{J}(\boldsymbol{h}, \boldsymbol{\rho}, \lambda)$:

$$\boldsymbol{J}(\boldsymbol{h}, \boldsymbol{\rho}, \lambda) = \begin{pmatrix} j_{11}(\boldsymbol{h}, \boldsymbol{\rho}, \lambda) & j_{12}(\boldsymbol{h}, \boldsymbol{\rho}, \lambda) \\ j_{21}(\boldsymbol{h}, \boldsymbol{\rho}, \lambda) & j_{22}(\boldsymbol{h}, \boldsymbol{\rho}, \lambda) \end{pmatrix}, \tag{3}$$

where $\boldsymbol{J}$ is the Jones matrix related to the optical path, which is a function of the object coordinate $\boldsymbol{h}$, aperture coordinate $\boldsymbol{\rho}$, and wavelength λ. The polarization aberration function $\boldsymbol{J}(\boldsymbol{h}, \boldsymbol{\rho}, \lambda)$ comprehensively describes the polarization characteristics of the optical system, where the phase term $\phi_0(\boldsymbol{h}, \boldsymbol{\rho}, \lambda)$ is related to the wave aberration function $W(\boldsymbol{h}, \boldsymbol{\rho}, \lambda)$ of geometrical optics as follows [9]:

$$W(\boldsymbol{h}, \boldsymbol{\rho}, \lambda) = \frac{\lambda}{2\pi}\phi_0(\boldsymbol{h}, \boldsymbol{\rho}, \lambda). \tag{4}$$

McGuire proposed the vector expression of the off-axis system polarization aberration in 1994 [9], which can represent the sum of the contributions of the optical elements in the system to the polarization aberration, (5), as shown at the bottom of the next page, where $P_{tuvwx} = \mathrm{A}_{tuvwx} + i\Phi_{tuvwx}$ is the polarization aberration coefficient; A_{tuvwx} and Φ_{tuvwx} are the real and imaginary parts of P_{tuvwx}, respectively; t represents the type of polarization behavior; u represents the order of dependence on the field of view $\boldsymbol{H}$; v represents the order of dependence on $\boldsymbol{\rho}$; and w represents the dependence on the angle ϕ in the entrance pupil coordinate (ρ, ϕ).

Pauli decomposed the polarization aberration function into amplitude aberration, phase aberration, diattenuation, and retardance [10]. The amplitude aberration is mainly related to the transmittance of the components in the system; therefore, it was not experimented in this study. However, the phase aberration is closely related to the optical path difference, which changes owing to the introduction of the freeform surface. Therefore, the effect of the freeform surface on the phase aberration cannot be neglected. Diattenuation and retardance are also related to factors such as the angle of incidence of light. Owing to the non-rotational symmetry of the freeform surface, the angle of incidence of light changes slightly. Therefore, the study of polarization aberrations in non-rotationally symmetric optical systems with freeform is essentially an in-depth analysis and calculation of phase aberrations, diattenuation, and retardance.

B. ESTABLISHMENT OF THE FREEFORM POLARIZATION ABERRATION ANALYSIS METHOD

The multi-degree-of-freedom characteristics of the freeform surface lead to different incidence angles of ray at various points on the interface. The introduction of freeform surface also changes the overall polarization matrix representation of the system. The traditional paraxial polarization aberration theory is used to analyze the polarization of the coaxial system, however, it is difficult to directly analyze the polarization characteristics of the freeform surface non-rotationally symmetric system. This study is based on fringe Zernike polynomials expression of freeform surfaces and analysis of the correlation between freeform surfaces and phase aberrations. We used the freeform surface polarization ray-tracing algorithm to obtain the diattenuation and retardance of the full-field of view and full aperture, and then analyzed the influence of freeform surfaces on the Jones matrix of the entire system.

1) PHASE ABERRATIONS INTRODUCED BY FREEFORM SURFACES

Zernike polynomials are chosen to represent freeform surfaces because of their ability to fit the full-field type of non-rotationally symmetric surfaces.

According to (4), it is observed that there is a quantitative relationship between wave and phase aberrations. The multiple degrees of freedom of the freeform surface shape will affect the optical path difference of the system to varying degrees, and then affect the wave aberration. Therefore, the freeform surface expressed by the fringe Zernike polynomial is related to the phase aberration through wave aberration. The expression of the Zernike polynomial is vectorized, and the aberration generated by the Zernike polynomial free surface is analyzed using the wave aberration theory. Further, we find the relationship between the Zernike freeform surface and the phase aberration. Thus, a phase aberration analysis method of the Zernike polynomial freeform surface was established. The specific process is as follows:

First, the Zernike polynomial, which was originally expressed in polar coordinates, is vectorized. The higher-order oscillation part of the Zernike polynomial freeform surface can be expressed as

$$C_i Z_i(\rho,\phi) = \begin{cases} C_x Z_x(\rho,\phi) \\ C_y Z_y(\rho,\phi), \end{cases} \tag{6}$$

where C_x and C_y are a set of Zernike polynomial coefficients. By transforming the Zernike polynomial and combining it with the vector multiplication rule, each group of coefficients in the Zernike polynomial can be vectorized to obtain

$$\boldsymbol{C_{x/y}} = C_{x/y} e^{im\alpha_{x/y}}, \tag{7}$$

where $C_{x/y}$ represents the magnitude of the coefficient vector, $\alpha_{x/y}$ represents the direction of the coefficient vector, and $\boldsymbol{m}$ represents the multiple of the Zernike polynomial azimuth angle ϕ. The specific relationship is as follows:

$$\begin{cases} \mathrm{C}_{x/y} = \sqrt{\mathrm{C}_x^2 + \mathrm{C}_y^2} \\ \alpha_{x/y} = \dfrac{\pi}{2} - \dfrac{1}{m}\arctan\left(\dfrac{C_y}{C_x}\right), \end{cases} \tag{8}$$

$\alpha_{x/y}$ has been modified. It is stipulated that $\alpha_{x/y}$ represents the angle of clockwise rotation from the +Y axis in the right-hand coordinate system.

Generally, the essence of wave aberration is caused by the optical path difference. Similarly, the nature of the wave aberration introduced by the freeform surface should also be caused by the optical path difference of the surface shape. Here, we take a reflective freeform surface as an example to illustrate the optical path difference produced by this surface, as shown in Fig. 1. When the angle of the incident light is not very large, the optical path lengths of the incident and outgoing rays are equivalent to the plane vector height of the incident point, and the optical path difference between the incident light and the outgoing light can be expressed as

$$\boldsymbol{\delta}_{x/y}(\boldsymbol{\rho}) = \frac{(n_2 - n_1)}{\lambda} \boldsymbol{C_{x/y}} \cdot Z(\boldsymbol{\rho}), \tag{9}$$

where n_1 and n_2 are the refractive indices of the medium where the incident and outgoing rays are located, λ is the wavelength, and $Z(\boldsymbol{\rho})$ is the Zernike polynomial vectorized according to the formula $\boldsymbol{\rho} = \rho \begin{pmatrix} \sin(\phi) \\ \cos(\phi) \end{pmatrix}$. For convenience,

$$J(H,\boldsymbol{\rho}) = \exp \begin{bmatrix} P_{00000}\boldsymbol{\sigma_0} + & \textit{constant piston} \\ P_{02000} H\cdot H\boldsymbol{\sigma_0} + & \textit{quadratic piston} \\ P_{01110} H\cdot\boldsymbol{\rho}\boldsymbol{\sigma_0} + & \textit{tilt} \\ P_{00200}\boldsymbol{\rho}\cdot\boldsymbol{\rho}\boldsymbol{\sigma_0} + & \textit{defocus} \\ P_{00400}(\boldsymbol{\rho}\cdot\boldsymbol{\rho})^2\boldsymbol{\sigma_0} + & \textit{spherical aberration} \\ P_{01310}(H\cdot\boldsymbol{\rho})(\boldsymbol{\rho}\cdot\boldsymbol{\rho})\boldsymbol{\sigma_0} + & \textit{coma} \\ P_{02200}(H\cdot H)(\boldsymbol{\rho}\cdot\boldsymbol{\rho})\boldsymbol{\sigma_0} + & \textit{field curvature} \\ \frac{1}{2}P_{02220}\left[(H\cdot H)(\boldsymbol{\rho}\cdot\boldsymbol{\rho}) + H^2\cdot\boldsymbol{\rho}^2\right]\boldsymbol{\sigma_0} + & \textit{astigmatism} \\ P_{03110}(H\cdot H)(H\cdot\boldsymbol{\rho})\boldsymbol{\sigma_0} + & \textit{distortion} \\ P_{04000}(H\cdot H)^2\boldsymbol{\sigma_0} + & \textit{quartic piston} \\ \textit{higher order terms} & \end{bmatrix} \tag{5}$$

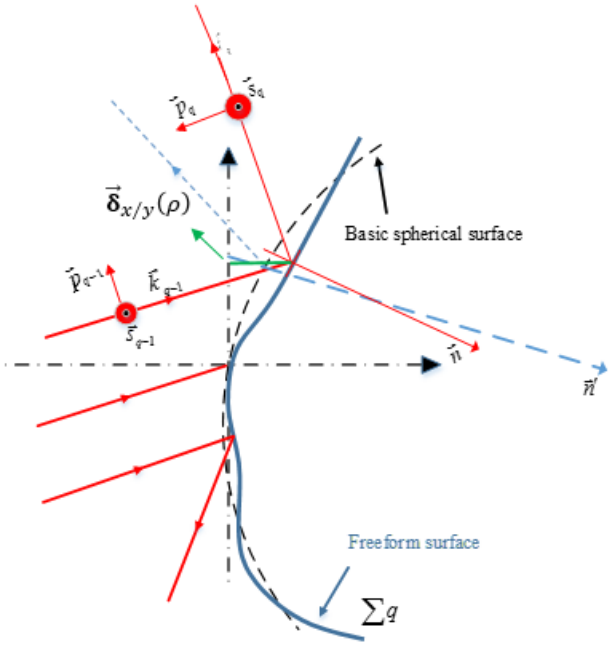

FIGURE 1. Schematic diagram of polarized light refraction, reflection, and optical path difference on the qth plane.

let $\boldsymbol{V}_{x/y} = \frac{(n_2-n_1)}{\lambda}\boldsymbol{C_{x/y}}$, then

$$\boldsymbol{\delta}_{x/y}(\boldsymbol{\rho}) = \boldsymbol{V}_{x/y} \cdot Z(\boldsymbol{\rho}). \tag{10}$$

According to the relationship between the phase term $\phi_0(\boldsymbol{h}, \boldsymbol{\rho}, \lambda)$ in the polarization aberration function $\boldsymbol{J}(\boldsymbol{h}, \boldsymbol{\rho}, \lambda)$ and the wave aberration function $W(\boldsymbol{h}, \boldsymbol{\rho}, \lambda)$ of geometric optics, $W(\boldsymbol{h}, \boldsymbol{\rho}, \lambda) = \frac{\lambda}{2\pi}\phi_0(\boldsymbol{h}, \boldsymbol{\rho}, \lambda)$. When the freeform surface is far from the diaphragm position, the contribution of the phase aberration is

$$\phi_0(\boldsymbol{h}, \boldsymbol{\rho}, \lambda) = \frac{2\pi}{\lambda}\boldsymbol{\delta}_{x/y}(\boldsymbol{\rho}). \tag{11}$$

It is worth noting that the wave aberration distribution of an optical system is closely related to the position of the diaphragm. Then the phase aberration distribution is also close to the diaphragm position. When the entrance pupil diameter is constant, and the diaphragm position is located on the spherical surface and away from the spherical surface, there is a pupil offset vector Δh between the two regions of the off-axis field of view incident on the mirror through the diaphragm. The pupil offset vector will redistribute the phase aberration of the optical system, as shown in (12):

$$\phi_0(\boldsymbol{\rho}) = \phi_0(\boldsymbol{\rho}' + \Delta\boldsymbol{h}). \tag{12}$$

When the field of view angle is not very large, it has a linear relationship with the offset vector, which can be expressed as

$$\Delta\boldsymbol{h} = \left(\frac{\bar{y}}{y}\right)\boldsymbol{H}, \tag{13}$$

where $\bar{y}$ represents the incident height of the chief ray of the off-axis field of view and y represents the height of the edge ray of the off-axis field of view.

When the position of the diaphragm coincides with the freeform surface, it can be regarded as a special case far from the position of the diaphragm. Concurrently, under the same caliber, the area where the light from each field of view enters the surface of the freeform surface is the same, and the surface shape has the same effect on the light of each field of view. Therefore, the contribution of the phase aberration generated by the freeform surface is independent of the field of view. When the diaphragm position is far from the freeform surface, Δh is related to the field of view vector $\boldsymbol{H}$. The phase aberration distribution generated by the freeform surface changes with the field of view. To analyze the influence of the freeform surface on the phase aberration distribution at any position in the optical system, a freeform surface phase aberration analytical formula far from the diaphragm position is derived.

When the freeform surface is far from the diaphragm position, the aperture of the light irradiated onto it is shifted. The aperture is shifted by vector Δh. The phase aberration contribution of the freeform surface will correspondingly become

$$\phi_0(\boldsymbol{h}, \boldsymbol{\rho}, \lambda) = \frac{2\pi}{\lambda}\boldsymbol{\delta}_{x/y}(\boldsymbol{\rho}) = \frac{2\pi}{\lambda}\boldsymbol{V}_{x/y} \cdot Z(\boldsymbol{\rho} + \Delta\boldsymbol{h}). \tag{14}$$

Equation (14) shows that although the Zernike polynomial is only related to the aperture, when it is far from the diaphragm position, its aberration contribution may also be related to the field of view.

This study focuses on the analysis of $Z_{5/6}$, the term of the striped Zernike polynomial. Owing to space constraints, the rest of the term will be analyzed in a subsequent paper.

The term expression of Zernike polynomial is

$$Z_{5/6}(\rho, \phi) = \begin{pmatrix} C_5\rho^2\cos(2\phi) \\ C_6\rho^2\sin(2\phi) \end{pmatrix}. \tag{15}$$

Let $\boldsymbol{\rho} = \rho\begin{pmatrix}\sin(\phi)\\ \cos(\phi)\end{pmatrix}$. Then, the expression of the $Z_{5/6}$ term of the Zernike polynomial can be written as

$$Z_{5/6}(\boldsymbol{\rho}) = \boldsymbol{\rho}^2. \tag{16}$$

According to the vector aberration theory, when the $Z_{5/6}$ term of the freeform surface is located far from the aperture stop, the vector wave aberration produced by the face-type vector height can be expressed as [11], [12]:

$$\begin{aligned}\boldsymbol{\delta}_{5/6,nonstop} &= \boldsymbol{V}_{5/6} \cdot (\boldsymbol{\rho} + \Delta\boldsymbol{h})^2 \\ &= \boldsymbol{V}_{5/6} \cdot \boldsymbol{\rho}^2 + 2\left(\frac{\bar{y}}{y}\right)\boldsymbol{V}_{5/6}\boldsymbol{H}^* \cdot \vec{\boldsymbol{\rho}} + \left(\frac{\bar{y}}{y}\right)^2\boldsymbol{V}_{5/6}\boldsymbol{H}^2,\end{aligned} \tag{17}$$

where

$$\begin{aligned}\boldsymbol{V}_{5/6} &= \frac{(n_2-n_1)}{\lambda}\sqrt{C_5^2 + C_6^2}e^{i2\alpha_{5/6}}, \\ \alpha_{5/6} &= \frac{\pi}{2} - \frac{1}{2}\arctan\left(\frac{C_6}{C_5}\right).\end{aligned}$$

From (4), $\phi_0(\boldsymbol{h}, \boldsymbol{\rho}, \lambda)$ varies as the wave aberration function $W(\boldsymbol{h}, \boldsymbol{\rho}, \lambda)$ varies. When the $Z_{5/6}$ term of the freeform

surface is far from the aperture stop, the expression of ϕ_0 is

$$\begin{aligned}&\phi_{\mathbf{0,5/6,}\boldsymbol{nonstop}}(\boldsymbol{h},\boldsymbol{\rho},\lambda)\\&=\frac{2\pi}{\lambda}\cdot\boldsymbol{\delta}_{\mathbf{5/6,}\boldsymbol{nonstop}}\\&=\frac{2\pi}{\lambda}\left[\boldsymbol{V}_{5/6}\cdot\boldsymbol{\rho}^2+2\left(\frac{\bar{y}}{y}\right)\boldsymbol{V}_{5/6}\boldsymbol{H}^*\cdot\vec{\boldsymbol{\rho}}+\left(\frac{\bar{\boldsymbol{y}}}{\boldsymbol{y}}\right)^2\boldsymbol{V}_{5/6}\boldsymbol{H}^2\right].\end{aligned}\tag{18}$$

It is evident from (18) that when the freeform surface of term $Z_{5/6}$ is far from the aperture stop position, it will produce polarization astigmatism, polarization tilt, and polarization translation terms. The latter two have no effect on imaging clarity and are not considered in this study. However, the polarization astigmatism term can be expressed as

$$\phi_{\mathbf{0,5/6,}\boldsymbol{nonstop,asti}}(\boldsymbol{h},\boldsymbol{\rho},\lambda)=\frac{2\pi}{\lambda}\boldsymbol{V}_{\mathbf{5/6}}\cdot\boldsymbol{\rho}^2.\tag{19}$$

It is evident from (5) that the inherent polarization astigmatism of the system is $\frac{1}{2}\Phi_{02220}\boldsymbol{H}^2\boldsymbol{\rho}^2$. When the $Z_{5/6}$ term of the freeform surface is far from the aperture stop position, the overall polarization astigmatism analytical expression of the optical system is

$$\begin{aligned}{}_{c5/6}\boldsymbol{P}_{asti}&=\frac{1}{2}\Phi_{02220}\boldsymbol{H}^2\boldsymbol{\rho}^2+\frac{2\boldsymbol{\pi}}{\lambda}\boldsymbol{V}_{5/6}\cdot\boldsymbol{\rho}^2\\&=\left(\frac{1}{2}\Phi_{02220}\boldsymbol{H}^2+\frac{2\boldsymbol{\pi}}{\lambda}\boldsymbol{V}_{5/6}\right)\cdot\boldsymbol{\rho}^2.\end{aligned}\tag{20}$$

C. DIATTENUATION AND RETARDANCE INTRODUCED BY FREEFORM SURFACES

The traditional polarization ray-tracing algorithm uses two-dimensional polarization ray tracing [13]–[15], which uses the Jones matrix to characterize the polarization properties of the optical interface [16]–[18]. Because the normal vector of each point on the freeform surface is different, the direction of the emitted ray corresponding to the light incident at different angles is also different. Adding the propagation vector $\boldsymbol{k}$ of the light to the traditional two-dimensional matrix can improve analysis of the polarization properties of optical systems containing freeform surfaces. In the following, based on the Zernike freeform surface expression method, a freeform surface polarization ray-tracing algorithm is constructed, and the influence of the freeform surface on the diattenuation and retardance is analyzed.

Freeform surface polarization ray-tracing is closely related to the light propagation vector $\boldsymbol{k}$. As shown in Fig. 1, the curvature is different at each point on the freeform. The angle of incidence differed at each point in the pupil. According to the Fresnel formula, the reflectance (refractive index) of the s and p components in the incident light changes at different angles. After the light passes through each optical element, the change in the s and p components changes the polarization state of the beam at the exit pupil. Therefore, the polarization characteristics of the system are closely related to the structure and film system parameters.

The Jones matrix added to the propagation vector $\boldsymbol{k}$ as a matrix $\boldsymbol{P_q}$ of 3×3, which represents the change in the polarization state when light passes through each interface of the optical system. In the global coordinate system, the polarization transformation matrix $\boldsymbol{P_{total}}$ representing the polarization transformation of the optical system for the incident light is obtained by tracing the freeform polarized ray.

$$\boldsymbol{E_{out}}=\boldsymbol{P_{total}}\cdot\boldsymbol{E_{in}},\tag{21}$$

where,

$$\boldsymbol{P_{total}}=\prod_{q=1}^{Q}\boldsymbol{P}_q\tag{22}$$

In (22), $\boldsymbol{E_{in}}$ and $\boldsymbol{E_{out}}$ represent the Jones vectors of the incident and emerging light beams, and the matrix $\boldsymbol{P_q}$ represents the change in the polarization state of the incident beam at the qth interface, as shown in Fig. 4. The relationship between $\boldsymbol{P_q}$ and $\boldsymbol{k}$, $\boldsymbol{s}$ and $\boldsymbol{p}$ components of the light beam at the optical interface is

$$\begin{aligned}\boldsymbol{P_q}=&\begin{pmatrix}s_{x,q}&p_{x,q}&k_{x,q}\\s_{y,q}&p_{y,q}&k_{y,q}\\s_{z,q}&p_{z,q}&k_{z,q}\end{pmatrix}\begin{pmatrix}a_{s,q}&0&0\\0&a_{p,q}&0\\0&0&1\end{pmatrix}\\&\begin{pmatrix}s_{x,q-1}&s_{y,q-1}&s_{z,q-1}\\p_{x,q-1}&p_{y,q-1}&p_{z,q-1}\\k_{x,q-1}&k_{y,q-1}&k_{z,q-1}\end{pmatrix},\end{aligned}\tag{23}$$

where $a_{s,q}$ and $a_{p,q}$ are the amplitude transmission (reflection) coefficients of the $\boldsymbol{s}$ and $\boldsymbol{p}$ components of the qth interface, respectively. $s_{m,q-1}$, $p_{m,q-1}$, and $k_{m,q-1}$ $(m=x,y,z)$ represent the coordinates of the $\boldsymbol{s},\boldsymbol{p}$ and $\boldsymbol{k}$ components of the incident light in the global coordinate system. $s_{n,q}$, $p_{n,q}$, and $k_{n,q}$ $(n=x,y,z)$ represent the coordinates of the $\boldsymbol{s}$, $\boldsymbol{p}$ and $\boldsymbol{k}$ components of the emerging light in the global coordinate system. The $\boldsymbol{s},\boldsymbol{p}$ components can be calculated using (24).

$$\begin{aligned}\boldsymbol{s}_{q-1}=\frac{\boldsymbol{k}_{q-1}\times\boldsymbol{k}_q}{\left|\boldsymbol{k}_{q-1}\times\boldsymbol{k}_q\right|},\quad\boldsymbol{p}_{q-1}=\boldsymbol{k}_{q-1}\times\boldsymbol{s}_{q-1},\\\boldsymbol{s}_q=\boldsymbol{s}_{q-1},\quad\boldsymbol{p}_q=\boldsymbol{k}_q\times\boldsymbol{s}_q.\end{aligned}\tag{24}$$

Then, the relationship between $\boldsymbol{P}$ and $\boldsymbol{k}$, $\boldsymbol{s}$ and $\boldsymbol{p}$ components of the beam at the interface of the freeform surface is

$$\begin{aligned}\boldsymbol{P}=&\begin{pmatrix}s_{x,1}&p_{x,1}&k_{x,1}\\s_{y,1}&p_{y,1}&k_{y,1}\\s_{z,1}&p_{z,1}&k_{z,1}\end{pmatrix}\begin{pmatrix}a_{s,1}&0&0\\0&a_{p,1}&0\\0&0&1\end{pmatrix}\\&\begin{pmatrix}s_{x,0}&s_{y,0}&s_{z,0}\\p_{x,0}&p_{y,0}&p_{z,0}\\k_{x,0}&k_{y,0}&k_{z,0}\end{pmatrix}.\end{aligned}\tag{25}$$

Employing the freeform surface polarization ray-tracing algorithm for the incident beam in a specific direction, the polarization conversion matrix $\boldsymbol{P_{total}}$ of the beam can be calculated for each interface of the system. The singular value

decomposition of $\boldsymbol{P_{total}}$ can be performed as follows.

$$\begin{aligned}\boldsymbol{P_{total}} &= \boldsymbol{UDV}^{\dagger} \\ &= \begin{bmatrix} k_{x,Q} & u_{x,1} & u_{x,2} \\ k_{y,Q} & u_{y,1} & u_{y,2} \\ k_{z,Q} & u_{z,1} & u_{z,2} \end{bmatrix} \begin{bmatrix} 1 & 0 & 0 \\ 0 & \Lambda_1 & 0 \\ 0 & 0 & \Lambda_2 \end{bmatrix} \\ &\quad \times \begin{bmatrix} k_{x,0} & k_{y,0} & k_{z,0} \\ v_{x,1} & v_{y,1} & v_{z,1} \\ v_{x,2} & v_{y,2} & v_{z,2} \end{bmatrix}. \end{aligned} \tag{26}$$

The polarization transformation matrix $\boldsymbol{P_{total}}$ is decomposed into two unitary matrices $\boldsymbol{U}, \boldsymbol{V}$ and a diagonal matrix $\boldsymbol{D}$. Λ_1 and Λ_2 ($\Lambda_1 \geq \Lambda_2$) contained in the diagonal matrix $\boldsymbol{D}$ are the eigenvalues of the polarization transformation matrix $\boldsymbol{P_{total}}$. $\boldsymbol{k_0}, \boldsymbol{k_Q}$ in the matrix correspond to the propagation direction of the incident light and the propagation direction of the emerging light after Q refraction and reflection. $\boldsymbol{v_1}\ \boldsymbol{v_2}$ and $\boldsymbol{u_1}\ \boldsymbol{u_2}$ correspond to the eigenpolarization states in the entrance pupil and the exit pupil of the optical system, respectively, and they satisfy the following relationship:

$$\boldsymbol{P_{total}} \cdot \boldsymbol{v}_1 = \Lambda_1 \boldsymbol{u}_1, \quad \boldsymbol{P_{total}} \cdot \boldsymbol{v}_2 = \Lambda_2 \boldsymbol{u}_2, \ \boldsymbol{P_{total}} \cdot \boldsymbol{k}_0 = \boldsymbol{k}_Q. \tag{27}$$

According to the definition of diattenuation and retardance [19], [20], The magnitude and direction of the diattenuation and retardance of the optical system can be calculated.

See Appendix A for the derivation of the polarization transmission matrix of the freeform optical system.

To show the influence of the freeform surface on the polarization aberration of the system, the polarization characteristics of a single-mirror system were studied. Suppose that the spherical radius of the reflector is 100 mm, the field of view angle is 2° and the aperture stop is placed at a distance of 100 mm from the front of the reflector then a $Z_{5/6}$ term of the freeform surface with a Zernike coefficient 5.5×10^{-4} is introduced on the reflector. The optical path of this system is illustrated in Fig. 2.

The freeform surface expression is shown in (28):

$$z = \frac{cr^2}{1 + \sqrt{1 - (1+k)\, c^2 r^2}} + \sum_{i=1}^{M} C_i Z_i\left(\rho, \phi\right), \tag{28}$$

where c is the spherical curvature, k is the quadratic coefficient, r is the radial aperture, and C_i is the Zernike coefficient corresponding to the i term of the Zernike polynomial.

Remember $K = \frac{cr^2}{1+\sqrt{1-(1+k)c^2r^2}}$, then $z = K + C_5 Z_5\left(\rho, \phi\right) + C_6 Z_6\left(\rho, \phi\right)$. The normal vector of the freeform surface can be expressed as: $n = \begin{bmatrix} n_x & n_y & n_z \end{bmatrix}^T$.

When the light is reflected on the mirror with the normal line $\begin{bmatrix} n_x & n_y & n_z \end{bmatrix}^T$, the transformation matrix of the light propagation direction is, (29), as shown at the bottom of the next page, where $\frac{\partial z_{5/6}}{\partial x} = \frac{\partial K}{\partial x} + C_5 \cdot \frac{\partial Z_5}{\partial x} + C_6 \cdot \frac{\partial Z_6}{\partial x}$, $\frac{\partial z_{5/6}}{\partial y} = \frac{\partial K}{\partial y} + C_5 \cdot \frac{\partial Z_5}{\partial y} + C_6 \cdot \frac{\partial Z_6}{\partial y}$. After the propagation vector $k_{in} = \begin{bmatrix} 0 & \sin 2^\circ & \cos 2^\circ \end{bmatrix}^T$ of the incident light beam passes

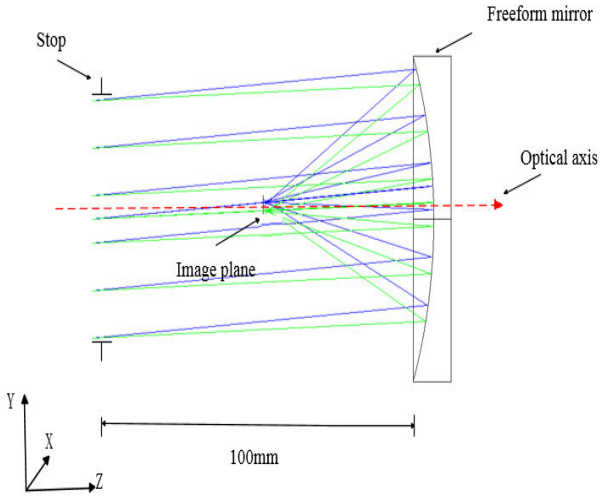

FIGURE 2. Schematic diagram of optical system.

through the optical system, the expression of the transmission vector of the outgoing light is

$$\begin{aligned}\boldsymbol{k_{out}} &= \begin{bmatrix} k_{out,x} \\ k_{out,y} \\ k_{out,z} \end{bmatrix} = H \cdot \boldsymbol{k_{in}} \\ &\approx \frac{1}{\left(\frac{\partial z_{5/6}}{\partial x}\right)^2 + \left(\frac{\partial z_{5/6}}{\partial y}\right)^2 + 1} \\ &\quad \times \begin{bmatrix} 2\frac{\partial z_{5/6}}{\partial x} \\ 2\frac{\partial z_{5/6}}{\partial y} \\ \left(\frac{\partial z_{5/6}}{\partial x}\right)^2 + \left(\frac{\partial z_{5/6}}{\partial y}\right)^2 - 1 \end{bmatrix}. \end{aligned}$$

According to (24), the components of $\boldsymbol{s}$ and $\boldsymbol{p}$ are expressed as follows:

$$\boldsymbol{s}_0 = \boldsymbol{s}_1 = \frac{1}{2\left(\frac{\partial z_{5/6}}{\partial x}\right)^2 + 2\left(\frac{\partial z_{5/6}}{\partial y}\right)^2} \begin{bmatrix} \frac{\partial z_{5/6}}{\partial y} \\ -\frac{\partial z_{5/6}}{\partial x} \\ 0 \end{bmatrix}, \tag{30}$$

$$\boldsymbol{p}_0 = \frac{1}{2\left(\frac{\partial z_{5/6}}{\partial x}\right)^2 + 2\left(\frac{\partial z_{5/6}}{\partial y}\right)^2} \begin{bmatrix} \frac{\partial z_{5/6}}{\partial x} \\ \frac{\partial z_{5/6}}{\partial y} \\ 0 \end{bmatrix}, \tag{31}$$

$$\boldsymbol{p}_1 = \begin{bmatrix} p_{x,1} \\ p_{y,1} \\ p_{z,1} \end{bmatrix}, \tag{32}$$

where

$$p_{x,1} = \frac{\left(\frac{\partial z_{5/6}}{\partial x}\right)^2 + \left(\frac{\partial z_{5/6}}{\partial y}\right)^2 - 1}{\left(\frac{\partial z_{5/6}}{\partial x}\right)^2 + \left(\frac{\partial z_{5/6}}{\partial y}\right)^2 + 1} \cdot \frac{\frac{\partial z_{5/6}}{\partial x}}{2\left(\frac{\partial z_{5/6}}{\partial x}\right)^2 + 2\left(\frac{\partial z_{5/6}}{\partial y}\right)^2},$$

$$p_{y,1} = \frac{\left(\frac{\partial z_{5/6}}{\partial x}\right)^2 + \left(\frac{\partial z_{5/6}}{\partial y}\right)^2 - 1}{\left(\frac{\partial z_{5/6}}{\partial x}\right)^2 + \left(\frac{\partial z_{5/6}}{\partial y}\right)^2 + 1} \cdot \frac{\frac{\partial z_{5/6}}{\partial y}}{2\left(\frac{\partial z_{5/6}}{\partial x}\right)^2 + 2\left(\frac{\partial z_{5/6}}{\partial y}\right)^2},$$

$$p_{z,1} = -\frac{1}{\left(\frac{\partial z_{5/6}}{\partial x}\right)^2 + \left(\frac{\partial z_{5/6}}{\partial y}\right)^2 + 1}.$$

Incorporating (30), (31), and (32) into (25), the freeform surface polarization transmission matrix expression of a single mirror system is, (33), as shown at the bottom of the next page.

The freeform surface polarization transmission matrix P_{total} of the system and the polarization state E_{out} of the outgoing light can be expressed as:

$$P_{total} = P, \tag{34}$$

$$E_{out} = P_{total} E_{in}. \tag{35}$$

The polarization transmission matrix of a freeform optical system is closely related to the Zernike polynomial. Diattenuation and retardance are obtained by the decomposition and transformation of the polarization transmission matrix. Therefore, the diattenuation and retardance are also affected by the freeform surface in the system. See Appendix B for the calculation of diattenuation and retardance of the freeform optical system.

III. ANALYSIS OF POLARIZATION DISTRIBUTION CHARACTERISTICS OF THE FREEFORM OPTICAL SYSTEM WITH OFF-AXIS FIELD OF VIEW

The traditional optical polarization aberration theory is based on paraxially polarized light, which is not suitable for analyzing the polarization aberration characteristics of non-rotationally symmetric systems containing freeform surfaces. In this section, we analyze the polarization aberration of a freeform optical system with an off-axis field of view. Although an optical system with an off-axis field of view is still a coaxial system in nature, it only uses the off-axis field of view for imaging. The aberration characteristics in the actual applicable field of view of the system are still non-rotationally symmetric. In this section, we combine the previously established freeform surface polarization aberration analysis method with fringe Zernike polynomials to analyze the phase aberration of the non-rotationally symmetric freeform surface optical system. Further, we will analyze the diattenuation and retardance characteristics of the system by freeform surface polarization ray-tracing.

The aberrations introduced by the freeform surface are different at the position of the system's aperture stop and at a position away from the aperture stop. To obtain generalized analysis results, the overall polarization aberration of the system with the Zernike term of the freeform surface at a position away from the aperture stop is analyzed as follows.

A. PHASE ABERRATION

First, the $Z_{5/6}$ term in the Zernike polynomial was analyzed. It is known from (18), that when the freeform surface is far from the aperture stop position, the polarization astigmatism term, which influences the system imaging, is mostly generated.

To verify the correctness of the aforementioned theoretical analysis, the polarization aberration distribution of a freeform surface single-reflector system was analyzed using optical software. The optical path of the system is shown in Fig. 2. Considering that the acquired data is completely obtained from the real ray tracing of the system, it can be used to verify the correctness of the theoretical derivation.

Different rays have different paths through the optical system, resulting in different Jones matrices for each light ray in the optical system. To characterize the polarization aberration properties of the entire optical system, the Jones matrix set of all rays from any one object point can be obtained at the exit pupil after passing through the optical system, by tracing the polarized rays through a full-aperture freeform surface.

$$\boldsymbol{J}(\boldsymbol{x},\boldsymbol{y}) = \begin{bmatrix} J_{XX}(x,y) & J_{XY}(x,y) \\ J_{YX}(x,y) & J_{YY}(x,y) \end{bmatrix} = \begin{bmatrix} A_{XX}(x,y)\, e^{i\varphi_{XX}(x,y)} & A_{XY}(x,y)\, e^{i\varphi_{XY}(x,y)} \\ A_{YX}(x,y)\, e^{i\varphi_{YX}(x,y)} & A_{YY}(x,y)\, e^{i\varphi_{YY}(x,y)} \end{bmatrix}, \tag{36}$$

$$H = \begin{bmatrix} 1-2n_x^2 & -2n_xn_y & -2n_xn_z \\ -2n_xn_y & 1-2n_y^2 & -2n_yn_z \\ -2n_xn_z & -2n_yn_z & 1-2n_z^2 \end{bmatrix} = \frac{1}{\left(\frac{\partial z_{5/6}}{\partial x}\right)^2 + \left(\frac{\partial z_{5/6}}{\partial y}\right)^2 + 1} \times \begin{bmatrix} -\left(\frac{\partial z_{5/6}}{\partial x}\right)^2 + \left(\frac{\partial z_{5/6}}{\partial y}\right)^2 + 1 & -2\frac{\partial z_{5/6}}{\partial x} \times \frac{\partial z_{5/6}}{\partial y} & 2\frac{\partial z_{5/6}}{\partial x} \\ -2\frac{\partial z_{5/6}}{\partial x} \times \frac{\partial z_{5/6}}{\partial y} & \left(\frac{\partial z_{5/6}}{\partial x}\right)^2 - \left(\frac{\partial z_{5/6}}{\partial y}\right)^2 + 1 & 2\frac{\partial z_{5/6}}{\partial y} \\ 2\frac{\partial z_{5/6}}{\partial x} & 2\frac{\partial z_{5/6}}{\partial y} & \left(\frac{\partial z_{5/6}}{\partial x}\right)^2 + \left(\frac{\partial z_{5/6}}{\partial y}\right)^2 - 1 \end{bmatrix} \tag{29}$$

where (x, y) denotes the coordinates of the intersection point between the light emitted from the object point and the exit pupil surface, as shown in Fig. 3. $E_{out} = J_{q-1} \cdots J_1 \cdot E_{in}$ shows the distributions of E_{in} and E_{out} represent the polarization states of the incident and outgoing light. The Jones matrix set, as shown in (36) is the Jones pupil, which characterizes the polarization state change of the light emitted by the object point from the entrance pupil to the exit pupil.

For the optical system shown in Fig. 2, the Jones pupil of the off-axis system of the field of view is calculated through polarization ray-tracing, as shown in Fig. 4, where the horizontal and vertical coordinates of each subplot represent the normalized X-axis and Y-axis coordinates of the exit pupil surface, respectively. Since the optical system shown in Fig. 2 is a single-mirror system with only one reflective surface, the Jones matrix of the reflective surface is the Jones matrix of the entire system. When light is reflected on the interface, the non-diagonal elements of the Jones matrix are 0. It can be seen that the magnitudes of A_{XX} and A_{YY} are close to 0.95, and the maximum value of A_{XX} is 0.958, which indicates that there is energy loss when the light is reflected in the optical system. The amplitudes of φ_{XX} and φ_{YY} are close to 0.28, which is caused by the phase aberration of the system. The freeform surface of the term $Z_{5/6}$ is removed. φ_{XX} and φ_{YY} are obtained through polarization ray tracing. The minimum values of φ_{XX} and φ_{YY} are changed, which shows that the introduction of the freeform surface of term $Z_{5/6}$ causes the phase aberration of the system to change.

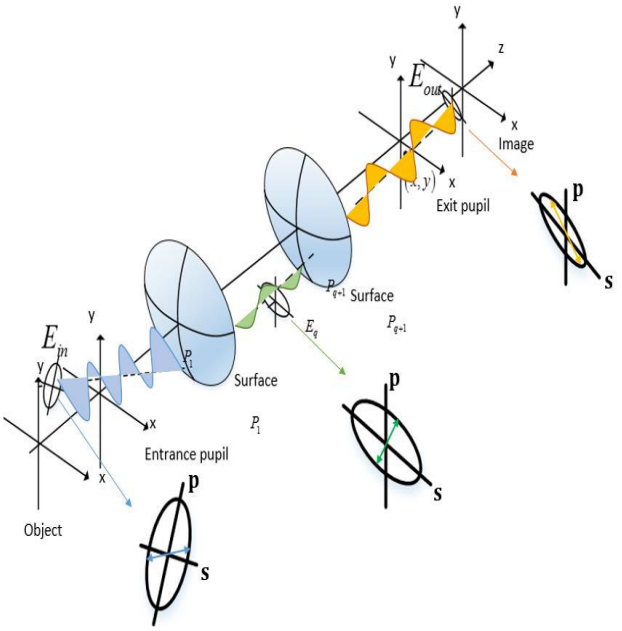

FIGURE 3. Schematic diagram of ray tracing.

$$\boldsymbol{P} = \begin{pmatrix} p_{11} & p_{12} & p_{13} \\ p_{21} & p_{22} & p_{23} \\ p_{31} & p_{32} & p_{33} \end{pmatrix},$$

$$p_{11} = \frac{\left(\frac{\partial z_{5/6}}{\partial y}\right)^2 a_{s,1}}{\left[2\left(\frac{\partial z_{5/6}}{\partial x}\right)^2 + 2\left(\frac{\partial z_{5/6}}{\partial y}\right)^2\right]^2} + \frac{\left(\frac{\partial z_{5/6}}{\partial x}\right)^2 + \left(\frac{\partial z_{5/6}}{\partial y}\right)^2 - 1}{\left(\frac{\partial z_{5/6}}{\partial x}\right)^2 + \left(\frac{\partial z_{5/6}}{\partial y}\right)^2 + 1} \cdot \frac{\left(\frac{\partial z_{5/6}}{\partial x}\right)^2 a_{p,1}}{\left[2\left(\frac{\partial z_{5/6}}{\partial x}\right)^2 + 2\left(\frac{\partial z_{5/6}}{\partial y}\right)^2\right]^2}$$

$$p_{12} = \frac{\frac{\partial z_{5/6}}{\partial x}\frac{\partial z_{5/6}}{\partial y} a_{s,1}}{\left[2\left(\frac{\partial z_{5/6}}{\partial x}\right)^2 + 2\left(\frac{\partial z_{5/6}}{\partial y}\right)^2\right]^2} + \frac{\left(\frac{\partial z_{5/6}}{\partial x}\right)^2 + \left(\frac{\partial z_{5/6}}{\partial y}\right)^2 - 1}{\left(\frac{\partial z_{5/6}}{\partial x}\right)^2 + \left(\frac{\partial z_{5/6}}{\partial y}\right)^2 + 1} \cdot \frac{\frac{\partial z_{5/6}}{\partial x}\frac{\partial z_{5/6}}{\partial y} a_{p,1}}{\left[2\left(\frac{\partial z_{5/6}}{\partial x}\right)^2 + 2\left(\frac{\partial z_{5/6}}{\partial y}\right)^2\right]^2},$$

$$p_{13} = \frac{2\frac{\partial z_{5/6}}{\partial x}}{\left(\frac{\partial z_{5/6}}{\partial x}\right)^2 + \left(\frac{\partial z_{5/6}}{\partial y}\right)^2 + 1}, \quad p_{21} = \frac{-\frac{\partial z_{5/6}}{\partial x}\frac{\partial z_{5/6}}{\partial y} a_{s,1}}{\left[2\left(\frac{\partial z_{5/6}}{\partial x}\right)^2 + 2\left(\frac{\partial z_{5/6}}{\partial y}\right)^2\right]^2} + \frac{\left(\frac{\partial z_{5/6}}{\partial x}\right)^2 + \left(\frac{\partial z_{5/6}}{\partial y}\right)^2 - 1}{\left(\frac{\partial z_{5/6}}{\partial x}\right)^2 + \left(\frac{\partial z_{5/6}}{\partial y}\right)^2 + 1} \cdot \frac{\frac{\partial z_{5/6}}{\partial y}\frac{\partial z_{5/6}}{\partial x} a_{p,1}}{\left[2\left(\frac{\partial z_{5/6}}{\partial x}\right)^2 + 2\left(\frac{\partial z_{5/6}}{\partial y}\right)^2\right]^2},$$

$$p_{22} = \frac{-\left(\frac{\partial z_{5/6}}{\partial x}\right)^2 a_{s,1}}{\left[2\left(\frac{\partial z_{5/6}}{\partial x}\right)^2 + 2\left(\frac{\partial z_{5/6}}{\partial y}\right)^2\right]^2} + \frac{\left(\frac{\partial z_{5/6}}{\partial x}\right)^2 + \left(\frac{\partial z_{5/6}}{\partial y}\right)^2 - 1}{\left(\frac{\partial z_{5/6}}{\partial x}\right)^2 + \left(\frac{\partial z_{5/6}}{\partial y}\right)^2 + 1} \cdot \frac{\left(\frac{\partial z_{5/6}}{\partial y}\right)^2 a_{p,1}}{\left[2\left(\frac{\partial z_{5/6}}{\partial x}\right)^2 + 2\left(\frac{\partial z_{5/6}}{\partial y}\right)^2\right]^2}, \quad p_{23} = \frac{2\frac{\partial z_{5/6}}{\partial y}}{\left(\frac{\partial z_{5/6}}{\partial x}\right)^2 + \left(\frac{\partial z_{5/6}}{\partial y}\right)^2 + 1},$$

$$p_{31} = -\frac{a_{p,1}}{\left(\frac{\partial z_{5/6}}{\partial x}\right)^2 + \left(\frac{\partial z_{5/6}}{\partial y}\right)^2 + 1} \frac{\frac{\partial z_{5/6}}{\partial x}}{2\left(\frac{\partial z_{5/6}}{\partial x}\right)^2 + 2\left(\frac{\partial z_{5/6}}{\partial y}\right)^2},$$

$$p_{32} = -\frac{a_{p,1}}{\left(\frac{\partial z_{5/6}}{\partial x}\right)^2 + \left(\frac{\partial z_{5/6}}{\partial y}\right)^2 + 1} \frac{\frac{\partial z_{5/6}}{\partial y}}{2\left(\frac{\partial z_{5/6}}{\partial x}\right)^2 + 2\left(\frac{\partial z_{5/6}}{\partial y}\right)^2}, \quad p_{33} = \frac{\left(\frac{\partial z_{5/6}}{\partial x}\right)^2 + \left(\frac{\partial z_{5/6}}{\partial y}\right)^2 - 1}{\left(\frac{\partial z_{5/6}}{\partial x}\right)^2 + \left(\frac{\partial z_{5/6}}{\partial y}\right)^2 + 1} \tag{33}$$

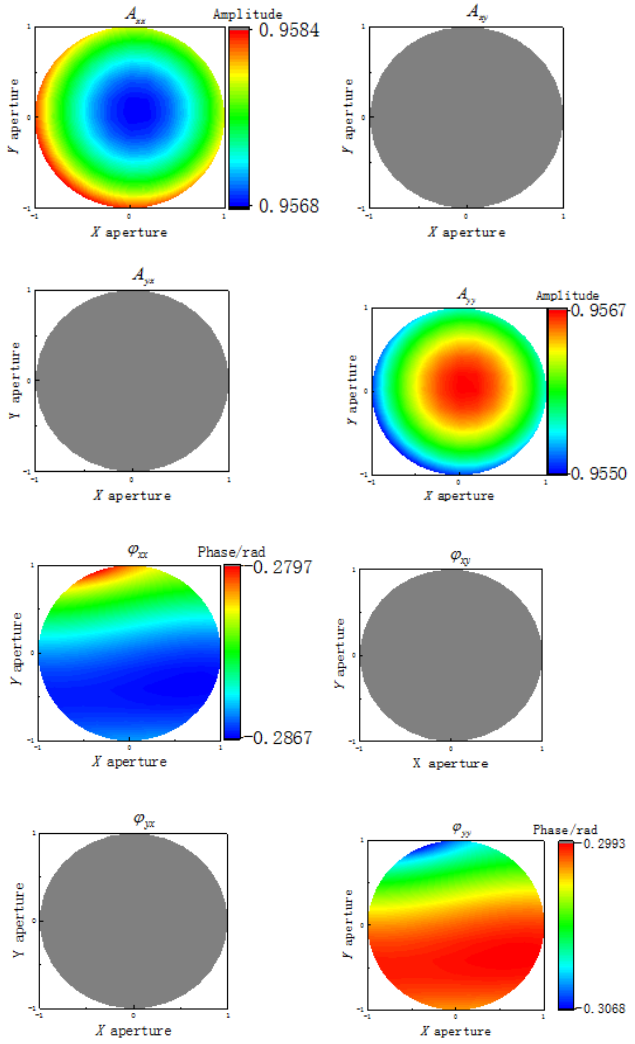

FIGURE 4. Jones pupil diagram with $Z_{5/6}$ term freeform.

From (2) and (3), $c_0 = \rho_0 + i\phi_0 = \frac{j_{11}(\vec{h},\vec{\rho},\lambda)+j_{22}(\vec{h},\vec{\rho},\lambda)}{2}$ is obtained, where ϕ_0 represents the phase aberration of the system. By tracing the set of Jones matrices of the optical system containing $Z_{5/6}$ term of the freeform and the one without the freeform, the phase aberration can be calculated. By marking the difference between the two, we can obtain the effect of introducing the $Z_{5/6}$ term of the freeform on the phase aberration ϕ_0. The difference is basically the same as the vector height diagram of the freeform surface, as shown in Fig. 5.

The field of view of this system is 2° off-axis on the Y-axis field of view, and $Z_{5/6}$ of the freeform surface is introduced with coefficients of 5.5×10^{-4}. As shown in Fig. 5, the rotation angle is $\alpha_{5/6} = \frac{3}{8}\pi$, and the influence of the $Z_{5/6}$ term of the freeform surface on the phase aberration mainly results in a change in astigmatism. The change in the phase aberration ϕ_0 is mainly reflected in the change in the polarization dispersion before and after the introduction of the freeform surface.

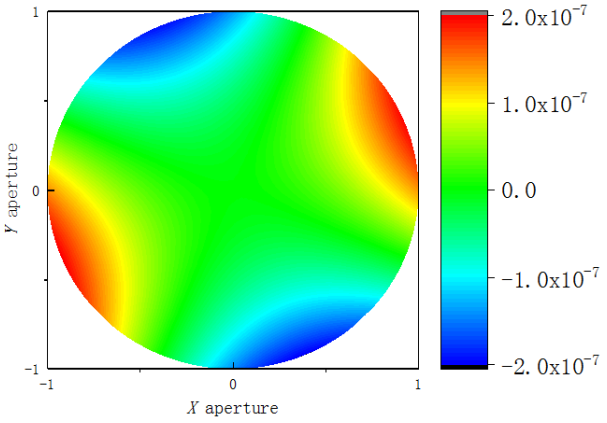

FIGURE 5. Effect of the freeform $Z_{5/6}$ term on the ϕ_0.

B. DIATTENUATION AND RETARDANCE

For the non-rotationally symmetric system shown in Fig. 2, the optical design software and MATLAB were used to trace the polarized ray of the full-aperture freeform system, and the polarization transformation matrix $\boldsymbol{P}_{total}$ is calculated for each ray at the exit pupil. The diattenuation and retardance of the corresponding point can be obtained by decomposing and transforming the singular value of the matrix $\boldsymbol{P}_{total}$, as shown in Fig. 6.

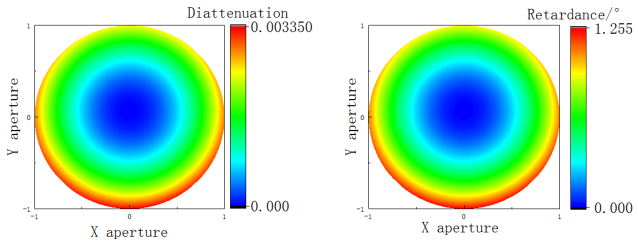

FIGURE 6. Distribution of polarization aberration of a freeform single reflection system with $Z_{5/6}$ term: (a) Diattenuation; (b) Retardance.

Fig. 6 shows that the diattenuation and retardance of the system both increase with the increase of the distance from the point to the optical axis, that is, the polarization effect of the optical system is evident in the off-axis field of view. The variation of polarization aberration is closely related to the structure of the optical system. The system is a non-rotationally symmetric system, and the off-axis direction is in the meridian plane. The diattenuation and retardance diagram of the system lose their rotational symmetry. In the non-rotationally symmetric optical system, the closer the incident parallel light is to the optical axis position, the smaller the angle of incidence in the optical system, and the smaller the corresponding amount of diattenuation and retardance.

To visually show the effect of the freeform surface on the diattenuation and retardance, the polarization aberration of the freeform surface system with the term $Z_{5/6}$ and the polarization aberration of the system without the freeform

surface are differentiated. The change in the diattenuation and retardance before and after the freeform surface is added was obtained as shown in Fig. 7.

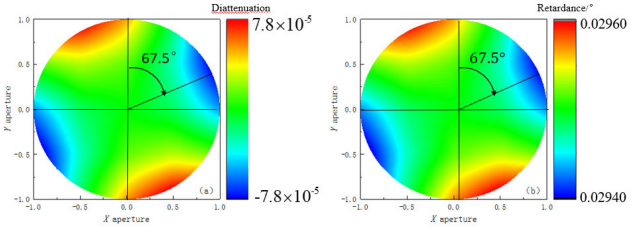

FIGURE 7. Changes in (a) diattenuation; (b) retardance before and after the freeform $Z_{5/6}$ is added.

As shown in Fig. 7, when the field of view is only shifted by 2° on the Y-axis, the freeform surface has an effect on both the attenuation and retardance. Its distribution law is the same as that of the freeform surface shape vector height diagram. The relationship between the rotation angle of the symmetry axis relative to the Y-axis and the coefficients of the Z_5 and Z_6 terms is $\alpha_{5/6} = \frac{\pi}{2} - \frac{1}{2}\arctan\left(\frac{C_6}{C_5}\right)$. To investigate the effect of the field of view angle on the polarization characteristics of the system, we set the coefficients of the A and S terms of the free-form surface in the system to $C_5 = 5.5 \times 10^{-4}$, $C_6 = 0$. The system is traced by the full-field polarized ray to obtain the Jones pupil, and then decomposed to obtain the diattenuation pupil (as shown in Fig. 8) and retardance pupil (as shown in Fig. 9) under the full field of view.

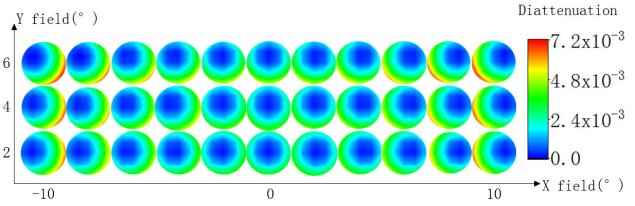

FIGURE 8. Diattenuation pupil in full field of view.

It can be seen from Figs. 8 and 9 that the diattenuation and retardance have the same distribution trend under different fields of view. From a horizontal point of view, taking the x = 0° field of view as the axis, the off-axis amount of the Y-axis field of view on the left and right sides is symmetrical. Therefore, the diattenuation and retardance distribution trends are also symmetrical. From a longitudinal point of view, the greater the off-axis amount of the field of view on the Y-axis, the greater the offset of the diattenuation and retardance. The maximum value in the pupil increases with an increase in the field of view. To further demonstrate the influence of the field of view on the polarization characteristics of freeform surfaces, the freeform surface was removed from the non-rotationally symmetric system, and full-field freeform polarization ray-tracing was carried out. The data of diattenuation and retardance were obtained under each field of view and compared with the data obtained when the freeform surface was included. The maximum changes in the diattenuation and retardance in each field of view by introducing the $Z_{5/6}$ term freeform surface were obtained, as shown in Fig. 10.

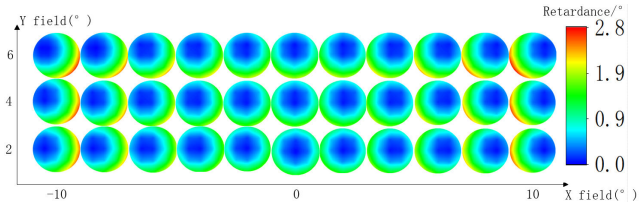

FIGURE 9. Retardance pupil in full field of view.

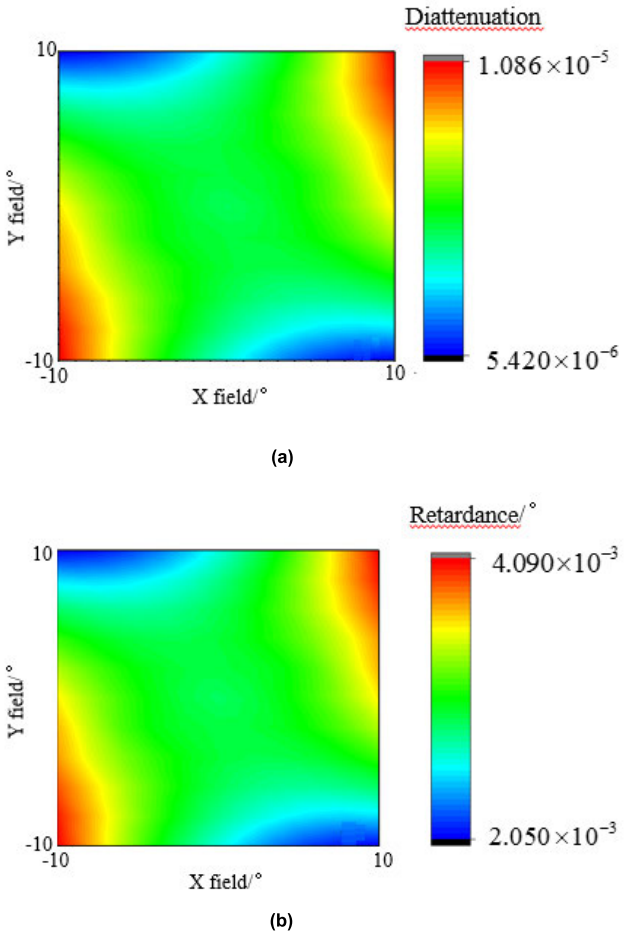

FIGURE 10. Effect of the freeform $Z_{5/6}$ term on the polarization aberration in full field of view (a) Diattenuation (b) Retardance.

The effect of the freeform surface on the polarization aberration under different fields of view is shown in Fig. 10. The introduction of the freeform surface has different degrees of influence on the polarization aberration in both the central and edge fields. The maximum change in the diattenuation is 9.5×10^{-5}, which changes 7.9% of the original diattenuation value, and the maximum change in retardance is 0.035°, which changes 8.5% of the original retardance value.

In the system design, the wavelength of the light source needs to be selected, in addition to setting the field of view and pupil parameters. Different wavelengths correspond to different complex refractive indices of metal surfaces in the system. The complex refractive indices of metals are expressed as $\boldsymbol{n} = n + \mathrm{i}k$, where n and k are positive real numbers. Among the common metals, Aluminum is usually chosen as the coating material of the reflectors [21], because the reflective principal of aluminum varies smoothly with wavelength, which also has good corrosion resistance. The complex refractive index of aluminum in the full-wave is shown in Fig. 11. Different complex refractive indices further affect the polarization characteristics of the system. Therefore, it is necessary to study the effect of wavelength on the polarization characteristics of the freeform surface. The polarization ray tracing of this single-reflector freeform system with full-hand is performed using Zemax, the ray is chosen which the field-of-view angle is 6° offset upward on the Y-axis only and the optical pupil coordinates is (0, 1). Then The Jones matrix under this ray is obtained and then it is decomposed to obtain the diattenuation and retardance at different wavelengths. Combined with the theoretical derivation in Appendix B for obtaining the diattenuation and retardance of the freeform optical system, the diattenuation and retardance of different wavelengths under the same incident light are obtained. As shown in Fig. 12 and 13.

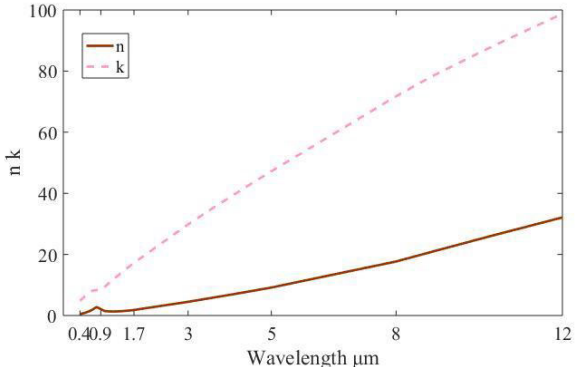

FIGURE 11. Complex refractive index $(\boldsymbol{n} + \mathrm{i}\boldsymbol{k})$ of Aluminium.

It can be seen from Fig. 12 and 13, that in the visible light wave (0.4-0.9), the diattenuation greatly increases with the growth of wavelength, while the retardance is opposite. Therefore, the polarization aberration caused by the system cannot be ignored when designing an optical system with aluminized coating in the visible light wave. In the near-infrared wave (0.9-1.7), both the diattenuation and retardance decrease with the growth of wavelength. In the infrared mid-wave (3-5) and long-wave (8-12), the wavelength has little effect on the diattenuation and retardance, and both tend to be stable with the increase of wavelength. Among them, the diattenuation is 0.0003, the retardance is 0.0545, and the polarization aberration is relatively small. Therefore, in the overall design of the infrared long-waveband system

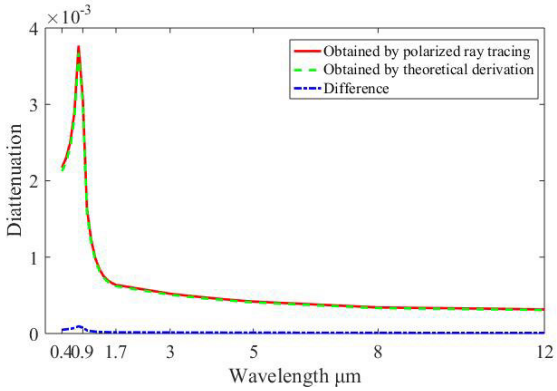

FIGURE 12. Change curve of diettenuation.

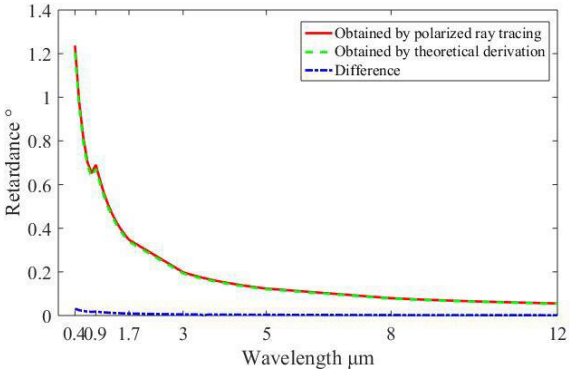

FIGURE 13. Change curve of retardance.

that the polarization is not highly required, the polarization characteristics of the system can not be given priority. Comparing the polarization aberrations obtained by freeform surface polarization theory and that obtained by Zemax polarization ray tracing under the full-wave, the maximum error of the diattenuation is 0.0307, and the error value is 2.55% of the diattenuation value obtained by Zemax real polarization ray tracing. The maximum error of retardance is 2.58% of the retardance value obtained by Zemax real polarization ray tracing. The correctness of the theory is further verified. The above simulation results show that the surface shape of the freeform surface affects the size and distribution of the polarization aberration.

IV. DESIGN AND POLARIZATION CHARACTERISTICS OF THE OFF-AXIS THREE-REFLECTION SYSTEM OF FIELD OF VIEW

To combine the theory with practical analysis and verify the results of the analysis, a large field-of-view off-axis three-mirror optical system is designed, and its polarization characteristics are analyzed in this section. The flow is shown in Fig. 14.

The steps are as follows: First, the parameters of the optical system in Zemax are obtained through the dynamic data connection mechanism in MATLAB. The aperture and field of view were equally divided. Second, a single field

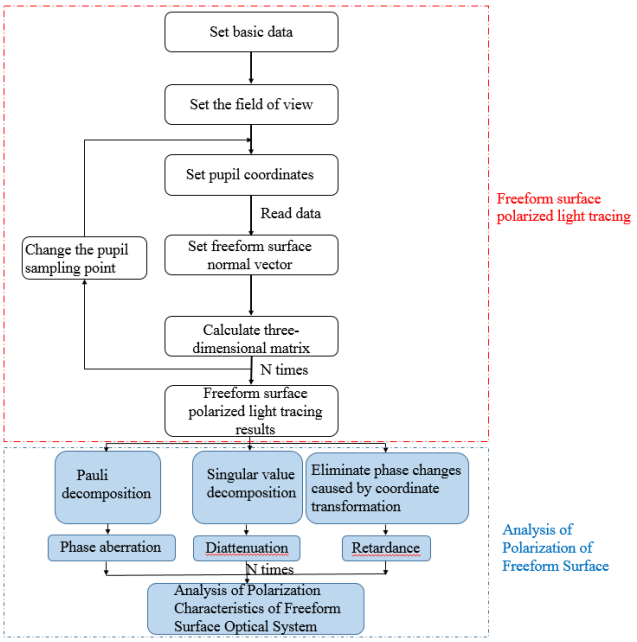

FIGURE 14. Analysis process of the polarization characteristics of the freeform surface optical system.

TABLE 1. Main optical indicators.

Specification	Parameters
Focal length	850 mm
F number	6.5
Field of view	20°*2°
Distortion	<0.5%
Pixel size	13um

of view point is selected and the polarization ray-tracing is performed for different optical pupil sampling points under this field of view to obtain the Jones pupil diagram and three-dimensional matrix under a single field of view. Third, the Pauli decomposition and singular value decomposition are performed to obtain the phase aberration, diattenuation, and retardance of the system under a single field of view. Fourth, the polarization characteristics of the system in the full field of view are obtained by switching the sampling points of the other fields of view, finally, the polarization characteristics of the optical system are analyzed.

To fully reflect the influence of the freeform surface shape on the distribution of polarization aberrations, the elements of the system are made free of eccentricity and tilt, and only the center of the system is eliminated using the off-axis method of the field of view. The optical specifications of the system are presented in Table 1.

The initial structure of the optical system was a three-piece secondary surface. To eliminate the influence of central occlusion and primary stray light, the edge field of view imaging was selected in the design, which led to the degradation of imaging quality, and also increased the polarization aberration of the system. To balance the level of aberration in the actual field of view, a freeform surface was introduced into the system, taking into account the effect of the freeform surface shape on each field of view. A freeform surface was also introduced on the primary mirror away from the aperture stop position. The initial structure was an optical system symmetrical about the Y-axis. In the selection of the field of view and the selection of the freeform surface, attention was paid to the problem of axis symmetry. Therefore, the freeform surface Z_5 term was selected to modulate the system. The simulation results in the previous section show that the surface shape of the freeform has a certain influence on the size of the polarization aberration. Considering that the field of view is 20° × 2°, the central field of view is shifted downwards by 8° on the Y-axis.

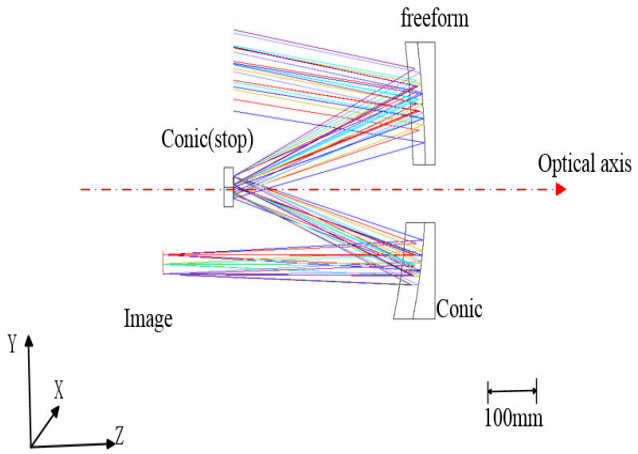

FIGURE 15. Optical system diagram.

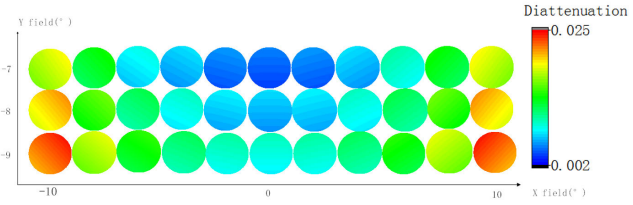

FIGURE 16. Diattenuation pupil in full field of view.

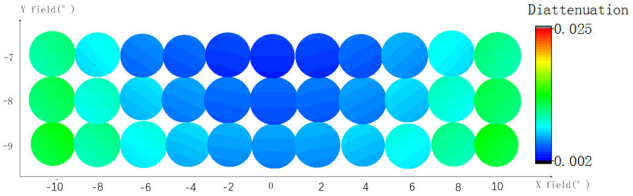

FIGURE 17. Diattenuation pupil of freeform surface in full field of view.

The distribution of the diattenuation and retardance of the system after the full-aperture freeform surface polarized ray tracing is shown in Fig. 16 and 18. The diattenuation and

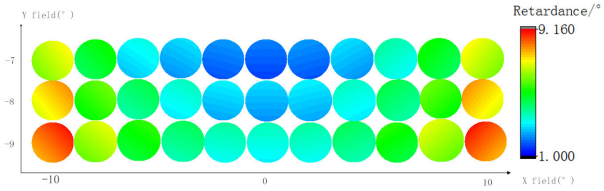

FIGURE 18. Retardance pupil in full field of view.

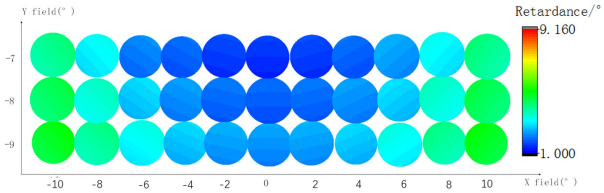

FIGURE 19. Retardance pupil of freeform surface in full field of view.

retardance caused by the freeform surface in the system were also calculated; they are shown in Fig. 17 and 19. The design results are consistent with the simulation results presented in section 3.2. The diattenuation and retardance distributions under different fields of view are the same, and their values increase with an increase in the field of view angle. The magnitude of the polarization aberration caused by the freeform surface accounts for 52.5% of the polarization aberration of the entire system. Therefore, the surface shape of the freeform surface affects the size and distribution of the overall polarization aberration of the system, and the polarization effect caused by it can reduce the imaging quality and measurement accuracy of the optical system. It is important to clarify the specific effect of the freeform surface shape on the polarization aberration to achieve modulation and constraint of the polarization aberration from the entire system. It is helpful to optimize the design of high-precision optical systems.

V. CONCLUSION

To quantitatively analyze the polarization aberration of non-rotationally symmetric optical systems with freeform surfaces, based on the Jones notation, a polarization aberration analytical model was constructed. For the freeform surface single reflection system with an off-axis field of view, the distribution characteristics of the phase aberration, diattenuation, and retardance at the exit pupil were obtained. The influence of the freeform surface on the Jones pupil of the entire system was visualized. Based on the polarization analysis of the freeform optical system, the Zernike coefficients were selected in a targeted manner, and a large-field off-axis three-mirror optical system with a freeform surface was designed. The design results showed that the introduction of the freeform surface not only affects the wave aberration, but also changes the Jones pupil distribution to varying degrees. This research was limited to freeform surfaces without eccentricity or tilt. In further studies, freeform optical systems with eccentricity and tilt should be analyzed to provide comprehensive guidance for the design of non-rotationally symmetric polarization imaging optical systems with freeform surfaces.

APPENDIX A
POLARIZATION TRANSMISSION MATRIX OF THE FREEFORM OPTICAL SYSTEM

After the propagation vector $k_{in} = \begin{bmatrix} 0 & \sin 2^\circ & \cos 2^\circ \end{bmatrix}^T$ of the incident light beam passes through the optical system, the expression of the transmission vector of the outgoing light is

$$\boldsymbol{k_{out}} = \begin{bmatrix} k_{out,x} \\ k_{out,y} \\ k_{out,z} \end{bmatrix} = H \cdot \boldsymbol{k_{in}} \approx \frac{1}{\left(\frac{\partial z}{\partial x}\right)^2 + \left(\frac{\partial z}{\partial y}\right)^2 + 1} \begin{bmatrix} 2\frac{\partial z}{\partial x} \\ 2\frac{\partial z}{\partial y} \\ \left(\frac{\partial z}{\partial x}\right)^2 + \left(\frac{\partial z}{\partial y}\right)^2 - 1 \end{bmatrix}.$$

According to (24), the components of $\boldsymbol{s}$ and $\boldsymbol{p}$ are expressed as follows:

$$\boldsymbol{s}_0 = \boldsymbol{s}_1 = \frac{1}{2\left(\frac{\partial z}{\partial x}\right)^2 + 2\left(\frac{\partial z}{\partial y}\right)^2} \begin{bmatrix} \frac{\partial z}{\partial y} \\ -\frac{\partial z}{\partial x} \\ 0 \end{bmatrix}, \tag{A1}$$

$$\boldsymbol{p}_0 = \frac{1}{2\left(\frac{\partial z}{\partial x}\right)^2 + 2\left(\frac{\partial z}{\partial y}\right)^2} \begin{bmatrix} \frac{\partial z}{\partial x} \\ \frac{\partial z}{\partial y} \\ 0 \end{bmatrix}. \tag{A2}$$

Taking the j-th surface in the optical system as an example, a freeform surface is added to the system.

The normal vector of the freeform surface is:

$$n = \begin{bmatrix} n_x \\ n_y \\ n_z \end{bmatrix} = \frac{1}{\sqrt{\left(\frac{\partial z}{\partial x}\right)^2 + \left(\frac{\partial z}{\partial y}\right)^2 + 1}} \begin{bmatrix} \frac{\partial z}{\partial x} \\ \frac{\partial z}{\partial y} \\ -1 \end{bmatrix}. \tag{A3}$$

When the light is reflected on the mirror with the normal line $\begin{bmatrix} n_x & n_y & n_z \end{bmatrix}^T$, the transformation matrix of the light propagation direction is, (A4), as shown at the bottom of the next page.

After the propagation vector $k_{in} = \begin{bmatrix} k_{in,x} & k_{in,y} & k_{in,z} \end{bmatrix}^T$ of the incident light beam passes through the optical system, the expression of the transmission vector of the outgoing light is, (A5), as shown at the bottom of the next page, the components of $\boldsymbol{s}$ and $\boldsymbol{p}$ are expressed as:

$$\begin{aligned} \boldsymbol{s}_0 = \boldsymbol{s}_1 &= \begin{bmatrix} s_x \\ s_y \\ s_z \end{bmatrix}, \\ \boldsymbol{p}_0 &= \begin{bmatrix} p_{x,0} \\ p_{y,0} \\ p_{z,0} \end{bmatrix} = k_{in} \times \boldsymbol{s}_0, \\ \boldsymbol{p}_1 &= \begin{bmatrix} p_{x,1} \\ p_{y,1} \\ p_{z,1} \end{bmatrix} = k_{out} \times \boldsymbol{s}_1, \end{aligned} \tag{A6}$$

where, s_x, s_y, s_z, $p_{x,0}$, $p_{y,0}$, $p_{z,0}$, $p_{x,1}$, $p_{y,1}$, and $p_{y,1}$, as shown at the bottom of the next page.

Then, the freeform surface polarization transmission matrix expression of the j-th surface in the optical system is

$$\boldsymbol{P} = \begin{pmatrix} s_{x,1} & p_{x,1} & k_{x,1} \\ s_{y,1} & p_{y,1} & k_{y,1} \\ s_{z,1} & p_{z,1} & k_{z,1} \end{pmatrix} \begin{pmatrix} a_{s,1} & 0 & 0 \\ 0 & a_{p,1} & 0 \\ 0 & 0 & 1 \end{pmatrix} \times \begin{pmatrix} s_{x,0} & s_{y,0} & s_{z,0} \\ p_{x,0} & p_{y,0} & p_{z,0} \\ k_{x,0} & k_{y,0} & k_{z,0} \end{pmatrix} \tag{A7}$$

APPENDIX B
The RETARDANCE AND DIATTENUATION OF THE FREEFORM OPTICAL SYSTEM

The expression of incident angle θ_1 can be obtained from (A3)and incident light $k_{in} = \begin{bmatrix} k_{in,x} & k_{in,y} & k_{in,z} \end{bmatrix}^T$ is

$$\cos\theta_1 = \frac{\vec{n}\cdot\vec{k}_{in}}{|\vec{n}|\cdot\left|\vec{k}_{in}\right|} = \frac{\frac{\partial z}{\partial x}\cdot k_{in,x} + \frac{\partial z}{\partial y}\cdot k_{in,y} - k_{in,z}}{\sqrt{\left(\frac{\partial z}{\partial x}\right)^2 + \left(\frac{\partial z}{\partial y}\right)^2 + 1}}. \tag{B1}$$

For light wave oblique into the metal interface:

$$\sin\theta_2 = \frac{1}{\tilde{n}}\sin\theta_1, \tag{B2}$$

where θ_2 is a complex number, which no longer has the meaning of the commonly understood angle of refraction. The expressions of $a_{s,1}$ and $a_{p,1}$ are

$$a_{s,1} = -\frac{\sin(\theta_1-\theta_2)}{\sin(\theta_1+\theta_2)}, \quad a_{p,1} = \frac{\tan(\theta_1-\theta_2)}{\tan(\theta_1+\theta_2)}. \tag{B3}$$

Perform singular value decomposition on P. Verified $a_{s,1}^2 \cdot \vec{s}_0 = \left(P^T\cdot P\right)\cdot\vec{s}_0$, $a_{p,1}^2\cdot\vec{p}_0 = \left(P^T\cdot P\right)\cdot\vec{p}_0$. Therefore, $a_{s,1}$ and $a_{p,1}$ are singular values of matrix P.

According to Taylor decomposition in the complex domain, we can get:

$$\begin{aligned} \sin x &= x - \frac{1}{3!}x^3 + o(x^3), \\ \cos x &= 1 - \frac{1}{2!}x^2 + o(x^2), \\ \tan x &= x + \frac{x^3}{3} + o(x^3). \end{aligned} \tag{B4}$$

Next, simplify $a_{s,1}$ and $a_{p,1}$, the expressions of $a_{s,1}$ and $a_{p,1}$ can be approximated:

$$\begin{aligned} a_{s,1} &= -\frac{\sin(\theta_1-\theta_2)}{\sin(\theta_1+\theta_2)} \approx -\frac{(\theta_1-\theta_2)\left[1-\frac{1}{6}(\theta_1-\theta_2)^2\right]}{(\theta_1+\theta_2)\left[1-\frac{1}{6}(\theta_1+\theta_2)^2\right]}, \\ a_{p,1} &= \frac{\tan(\theta_1-\theta_2)}{\tan(\theta_1+\theta_2)} \approx \frac{(\theta_1-\theta_2)+\frac{1}{3}(\theta_1-\theta_2)^3}{(\theta_1+\theta_2)+\frac{1}{3}(\theta_1+\theta_2)^3}. \end{aligned} \tag{B5}$$

Apply Taylor decomposition (B4) to (B1) and (B2), and bring it into (B5) to obtain:

$$\begin{aligned} a_{s,1} &\approx -\frac{0.97-i}{7.17+i} = \left|a_{s,1}\right| e^{i\varphi_{s,1}}, \\ a_{p,1} &\approx \frac{0.97-i}{7.17+i}\cdot\frac{7.07+(0.97-\mathrm{i})\mathrm{Q}}{7.07+(7.17-\mathrm{i})\mathrm{Q}} = \left|a_{p,1}\right| e^{i\varphi_{p,1}}, \end{aligned} \tag{B6}$$

where $\mathrm{Q} = \sqrt{2 - 2\frac{\frac{\partial z}{\partial x}\cdot k_{in,x} + \frac{\partial z}{\partial y}\cdot k_{in,y} - k_{in,z}}{\sqrt{\left(\frac{\partial z}{\partial x}\right)^2 + \left(\frac{\partial z}{\partial y}\right)^2 + 1}}}$.

$$H = \begin{bmatrix} 1-2n_x^2 & -2n_xn_y & -2n_xn_z \\ -2n_xn_y & 1-2n_y^2 & -2n_yn_z \\ -2n_xn_z & -2n_yn_z & 1-2n_z^2 \end{bmatrix} = \frac{1}{\left(\frac{\partial z}{\partial x}\right)^2 + \left(\frac{\partial z}{\partial y}\right)^2 + 1} \times \begin{bmatrix} -\left(\frac{\partial z}{\partial x}\right)^2 + \left(\frac{\partial z}{\partial y}\right)^2 + 1 & -2\frac{\partial z}{\partial x}\times\frac{\partial z}{\partial y} & 2\frac{\partial z}{\partial x} \\ -2\frac{\partial z}{\partial x}\times\frac{\partial z}{\partial y} & \left(\frac{\partial z}{\partial x}\right)^2 - \left(\frac{\partial z}{\partial y}\right)^2 + 1 & 2\frac{\partial z}{\partial y} \\ 2\frac{\partial z}{\partial x} & 2\frac{\partial z}{\partial y} & \left(\frac{\partial z}{\partial x}\right)^2 + \left(\frac{\partial z}{\partial y}\right)^2 - 1 \end{bmatrix} \tag{A4}$$

$$\boldsymbol{k_{out}} = \begin{bmatrix} k_{out,x} \\ k_{out,y} \\ k_{out,z} \end{bmatrix} = H\cdot\boldsymbol{k_{in}} = \frac{1}{\left(\frac{\partial z}{\partial x}\right)^2 + \left(\frac{\partial z}{\partial y}\right)^2 + 1} \begin{bmatrix} \left[-\left(\frac{\partial z}{\partial x}\right)^2 + \left(\frac{\partial z}{\partial y}\right)^2 + 1\right]k_{in,x} + \left(-2\frac{\partial z}{\partial x}\times\frac{\partial z}{\partial y}\right)k_{in,y} + \left(2\frac{\partial z}{\partial x}\right)k_{in,z} \\ \left(-2\frac{\partial z}{\partial x}\times\frac{\partial z}{\partial y}\right)k_{in,x} + \left[\left(\frac{\partial z}{\partial x}\right)^2 - \left(\frac{\partial z}{\partial y}\right)^2 + 1\right]k_{in,y} + \left(2\frac{\partial z}{\partial y}\right)k_{in,z} \\ \left(2\frac{\partial z}{\partial x}\right)k_{in,x} + \left(2\frac{\partial z}{\partial y}\right)k_{in,y} + \left[\left(\frac{\partial z}{\partial x}\right)^2 + \left(\frac{\partial z}{\partial y}\right)^2 - 1\right]k_{in,z} \end{bmatrix} \tag{A5}$$

$$
\begin{aligned}
s_x &= \left(-2\frac{\partial z}{\partial x}\times\frac{\partial z}{\partial y}\right)k_{in,x}k_{in,z}+\left[-2\left(\frac{\partial z}{\partial y}\right)^2+2\right]k_{in,y}k_{in,z}+\left(2\frac{\partial z}{\partial y}\right)k_{in,z}^2-\left(2\frac{\partial z}{\partial x}\right)k_{in,x}k_{in,y}-\left(2\frac{\partial z}{\partial y}\right)k_{in,y}^2,\\
s_y &= \left(2\frac{\partial z}{\partial x}\right)k_{in,x}^2+\left(2\frac{\partial z}{\partial y}\right)k_{in,x}k_{in,y}+\left[2\left(\frac{\partial z}{\partial x}\right)^2-2\right]k_{in,x}k_{in,z}+\left(2\frac{\partial z}{\partial x}\times\frac{\partial z}{\partial y}\right)k_{in,y}k_{in,z}-\left(2\frac{\partial z}{\partial x}\right)k_{in,z}^2,\\
s_z &= \left[-2\left(\frac{\partial z}{\partial x}\right)^2+2\left(\frac{\partial z}{\partial y}\right)^2\right]k_{in,x}k_{in,y}+\left(-2\frac{\partial z}{\partial x}\times\frac{\partial z}{\partial y}\right)k_{in,y}^2+\left(2\frac{\partial z}{\partial x}\right)k_{in,y}k_{in,z}+\left(2\frac{\partial z}{\partial x}\times\frac{\partial z}{\partial y}\right)k_{in,x}k_{in,x}-\left(2\frac{\partial z}{\partial y}\right)k_{in,x}k_{in,z},\\
p_{x,0} &= \left\{\left[-2\left(\frac{\partial z}{\partial x}\right)^2+2\left(\frac{\partial z}{\partial y}\right)^2\right]k_{in,x}k_{in,y}^2+\left(-2\frac{\partial z}{\partial x}\times\frac{\partial z}{\partial y}\right)k_{in,y}^3+\left(2\frac{\partial z}{\partial x}\right)k_{in,y}^2k_{in,z}\right\}\\
&\quad-\left[\left(-2\frac{\partial z}{\partial x}\times\frac{\partial z}{\partial y}\right)k_{in,x}^2k_{in,y}+\left(4\frac{\partial z}{\partial y}\right)k_{in,x}k_{in,y}k_{in,z}\right]\\
&\quad-\left\{\left(2\frac{\partial z}{\partial x}\right)k_{in,x}^2k_{in,z}+\left[2\left(\frac{\partial z}{\partial x}\right)^2-2\right]k_{in,x}k_{in,z}^2\right\}+\left[\left(-2\frac{\partial z}{\partial x}\times\frac{\partial z}{\partial y}\right)k_{in,y}k_{in,z}^2+\left(2\frac{\partial z}{\partial x}\right)k_{in,z}^3\right],\\
p_{y,0} &= \left[\left(-2\frac{\partial z}{\partial x}\times\frac{\partial z}{\partial y}\right)k_{in,x}^2k_{in,y}+\left(2\frac{\partial z}{\partial y}-2\frac{\partial z}{\partial x}\right)k_{in,x}k_{in,y}k_{in,z}\right]\\
&\quad-\left\{\left[2\left(\frac{\partial z}{\partial y}\right)^2-2\left(\frac{\partial z}{\partial x}\right)^2\right]k_{in,x}k_{in,y}^2+\left(-2\frac{\partial z}{\partial x}\times\frac{\partial z}{\partial y}\right)k_{in,y}^3+\left(2\frac{\partial z}{\partial y}+2\frac{\partial z}{\partial x}\right)k_{in,y}^2k_{in,z}\right\}\\
&\quad+\left\{\left(-2\frac{\partial z}{\partial x}\times\frac{\partial z}{\partial y}\right)k_{in,x}k_{in,z}^2+\left[-2\left(\frac{\partial z}{\partial y}\right)^2+2\right]k_{in,y}k_{in,z}^2+\left(2\frac{\partial z}{\partial y}\right)k_{in,z}^3\right\},\\
p_{z,0} &= \left\{\left(2\frac{\partial z}{\partial x}\right)k_{in,x}^3+\left(2\frac{\partial z}{\partial y}-2\frac{\partial z}{\partial x}\times\frac{\partial z}{\partial y}\right)k_{in,x}^2k_{in,y}+\left[2\left(\frac{\partial z}{\partial x}\right)^2-2\right]k_{in,x}^2k_{in,z}\right\}\\
&\quad-\left[\left(2\frac{\partial z}{\partial y}-2\frac{\partial z}{\partial x}\times\frac{\partial z}{\partial y}\right)k_{in,x}k_{in,y}k_{in,z}+\left(2\frac{\partial z}{\partial x}\right)k_{in,x}k_{in,z}^2\right]\\
&\quad-\left\{\left[-2\left(\frac{\partial z}{\partial x}\right)^2+2\left(\frac{\partial z}{\partial y}\right)^2\right]k_{in,x}k_{in,y}^2+\left(-2\frac{\partial z}{\partial x}\times\frac{\partial z}{\partial y}\right)k_{in,y}^3+\left(2\frac{\partial z}{\partial x}\right)k_{in,y}^2k_{in,z}\right\},\\
p_{x,1} &= \frac{1}{\left(\frac{\partial z}{\partial x}\right)^2+\left(\frac{\partial z}{\partial y}\right)^2+1}\left\{\left(-2\frac{\partial z}{\partial x}\times\frac{\partial z}{\partial y}\right)k_{in,x}+\left[\left(\frac{\partial z}{\partial x}\right)^2-\left(\frac{\partial z}{\partial y}\right)^2+1\right]k_{in,y}+\left(2\frac{\partial z}{\partial y}\right)k_{in,z}\right\}\\
&\quad\times\left\{\left[-2\left(\frac{\partial z}{\partial x}\right)^2+2\left(\frac{\partial z}{\partial y}\right)^2\right]k_{in,x}k_{in,y}+\left(-2\frac{\partial z}{\partial x}\times\frac{\partial z}{\partial y}\right)k_{in,y}^2+\left(2\frac{\partial z}{\partial x}\right)k_{in,y}k_{in,z}\right.\\
&\quad\left.+\left(2\frac{\partial z}{\partial x}\times\frac{\partial z}{\partial y}\right)k_{in,x}k_{in,x}-\left(2\frac{\partial z}{\partial y}\right)k_{in,x}k_{in,z}\right\}\\
&\quad-\frac{1}{\left(\frac{\partial z}{\partial x}\right)^2+\left(\frac{\partial z}{\partial y}\right)^2+1}\left\{\left(2\frac{\partial z}{\partial x}\right)k_{in,x}+\left(2\frac{\partial z}{\partial y}\right)k_{in,y}+\left[\left(\frac{\partial z}{\partial x}\right)^2+\left(\frac{\partial z}{\partial y}\right)^2-1\right]k_{in,z}\right\}\\
&\quad\times\left\{\left(2\frac{\partial z}{\partial x}\right)k_{in,x}^2+\left(2\frac{\partial z}{\partial y}\right)k_{in,x}k_{in,y}+\left[2\left(\frac{\partial z}{\partial x}\right)^2-2\right]k_{in,x}k_{in,z}+\left(2\frac{\partial z}{\partial x}\times\frac{\partial z}{\partial y}\right)k_{in,y}k_{in,z}-\left(2\frac{\partial z}{\partial x}\right)k_{in,z}^2\right\},\\
p_{y,1} &= \frac{1}{\left(\frac{\partial z}{\partial x}\right)^2+\left(\frac{\partial z}{\partial y}\right)^2+1}\left\{\left(2\frac{\partial z}{\partial x}\right)k_{in,x}+\left(2\frac{\partial z}{\partial y}\right)k_{in,y}+\left[\left(\frac{\partial z}{\partial x}\right)^2+\left(\frac{\partial z}{\partial y}\right)^2-1\right]k_{in,z}\right\}\\
&\quad\times\left\{\left(-2\frac{\partial z}{\partial x}\times\frac{\partial z}{\partial y}\right)k_{in,x}k_{in,z}+\left[-2\left(\frac{\partial z}{\partial y}\right)^2+2\right]k_{in,y}k_{in,z}+\left(2\frac{\partial z}{\partial y}\right)k_{in,z}^2-\left(2\frac{\partial z}{\partial x}\right)k_{in,x}k_{in,y}-\left(2\frac{\partial z}{\partial y}\right)k_{in,y}^2\right\}\\
&\quad-\frac{1}{\left(\frac{\partial z}{\partial x}\right)^2+\left(\frac{\partial z}{\partial y}\right)^2+1}\left\{\left[-\left(\frac{\partial z}{\partial x}\right)^2+\left(\frac{\partial z}{\partial y}\right)^2+1\right]k_{in,x}+\left(-2\frac{\partial z}{\partial x}\times\frac{\partial z}{\partial y}\right)k_{in,y}+\left(2\frac{\partial z}{\partial x}\right)k_{in,z}\right\}\\
&\quad\times\left\{\left[-2\left(\frac{\partial z}{\partial x}\right)^2+2\left(\frac{\partial z}{\partial y}\right)^2\right]k_{in,x}k_{in,y}+\left(-2\frac{\partial z}{\partial x}\times\frac{\partial z}{\partial y}\right)k_{in,y}^2+\left(2\frac{\partial z}{\partial x}\right)k_{in,y}k_{in,z}\right.\\
&\quad\left.+\left(2\frac{\partial z}{\partial x}\times\frac{\partial z}{\partial y}\right)k_{in,x}k_{in,x}-\left(2\frac{\partial z}{\partial y}\right)k_{in,x}k_{in,z}\right\},\\
p_{y,1} &= \frac{1}{\left(\frac{\partial z}{\partial x}\right)^2+\left(\frac{\partial z}{\partial y}\right)^2+1}\left\{\left(2\frac{\partial z}{\partial x}\right)k_{in,x}+\left(2\frac{\partial z}{\partial y}\right)k_{in,y}+\left[\left(\frac{\partial z}{\partial x}\right)^2+\left(\frac{\partial z}{\partial y}\right)^2-1\right]k_{in,z}\right\}\\
&\quad\times\left\{\left(-2\frac{\partial z}{\partial x}\times\frac{\partial z}{\partial y}\right)k_{in,x}k_{in,z}+\left[-2\left(\frac{\partial z}{\partial y}\right)^2+2\right]k_{in,y}k_{in,z}+\left(2\frac{\partial z}{\partial y}\right)k_{in,z}^2-\left(2\frac{\partial z}{\partial x}\right)k_{in,x}k_{in,y}-\left(2\frac{\partial z}{\partial y}\right)k_{in,y}^2\right\}\\
&\quad-\frac{1}{\left(\frac{\partial z}{\partial x}\right)^2+\left(\frac{\partial z}{\partial y}\right)^2+1}\left\{\left[-\left(\frac{\partial z}{\partial x}\right)^2+\left(\frac{\partial z}{\partial y}\right)^2+1\right]k_{in,x}+\left(-2\frac{\partial z}{\partial x}\times\frac{\partial z}{\partial y}\right)k_{in,y}+\left(2\frac{\partial z}{\partial x}\right)k_{in,z}\right\}\\
&\quad\times\left\{\left[-2\left(\frac{\partial z}{\partial x}\right)^2+2\left(\frac{\partial z}{\partial y}\right)^2\right]k_{in,x}k_{in,y}+\left(-2\frac{\partial z}{\partial x}\times\frac{\partial z}{\partial y}\right)k_{in,y}^2+\left(2\frac{\partial z}{\partial x}\right)k_{in,y}k_{in,z}\right.\\
&\quad\left.+\left(2\frac{\partial z}{\partial x}\times\frac{\partial z}{\partial y}\right)k_{in,x}k_{in,x}-\left(2\frac{\partial z}{\partial y}\right)k_{in,x}k_{in,z}\right\}
\end{aligned}
$$

According to the definition of retardance, and diattenuation, we can obtain:

$$D = \frac{|a_{s,1}|^2 - |a_{p,1}|^2}{|a_{s,1}|^2 + |a_{p,1}|^2},$$
$$\delta = \varphi_{s,1} - \varphi_{p,1}. \tag{B7}$$

ACKNOWLEDGMENT

Yilan Zhang would like to thank her tutor—Huilin Jiang, a Lecturer with the School of Optical Engineering. In the process of composing this article, he gave many academic and constructive advices, which helped her to correct this article. At the same time, Yilan Zhang would like to appreciate her teacher Haodong Shi, who gave useful professional knowledge and information in this article. At last, Yilan Zhang is very grateful to her dear friends, Miao Xu and Jiayu Wang, who offered her the confidence and discussed with her about this article. Of course, she would like to thank her father, Lianlin Zhang, and her mother, Cuiju Li, because of their warm care.

REFERENCES

[1] J. B. Breckinridge, T. Wai Size Lam, and R. A. Chipman, "Polarization aberration in astronomical telescopes," *Publications Astronomical Soc. Pacific*, vol. 127, p. 445, May 2015.
[2] R. A. Chipman, *Polarization Aberrations*. Tucson, AZ, USA: Univ. Arizona, 1987.
[3] J. P. McGuire and R. A. Chipman, "Polarization aberrations 1 rotationally symmetric optical systems," *Appl. Opt.*, vol. 33, no. 22, p. 5080, Aug. 1994.
[4] J. Sasián, "Polarization fields and wavefronts of two sheets for understanding polarization aberrations in optical imaging systems," *Opt. Eng.*, vol. 53, no. 3, Mar. 2014, Art. no. 035102.
[5] H. Wang, L. Zheng, M. Yan, J. Wang, S. Qu, and R. Luo, "Design and analysis of miniaturized low profile and second-order multi-band polarization selective surface for multipath communication application," *IEEE Access*, vol. 7, pp. 13455–13467, 2019.
[6] Z. Ding, Y. Yao, X. S. Yao, X. Chen, C. Wang, S. Wang, and T. Liu, "Demonstration of compact *in situ* Mueller-matrix polarimetry based on binary polarization rotators," *IEEE Access*, vol. 7, pp. 144561–144571, 2019.
[7] X. R. Xu, W. Huang, and M. F. Xu, "Orthogonal polynomials describing polarization aberration for rotationally symmetric optical systems," *Opt. Exp.*, vol. 23, no. 21, 2015, Art. no. 248659.
[8] J. P. McGuire and R. A. Chipman, "Polarization aberrations 2 tilted and decentered optical systems," *Appl. Opt.*, vol. 33, no. 22, p. 5101, Aug. 1994.
[9] R. A. Chipman, "Polarization analysis of optical systems," *Opt. Eng.*, vol. 28, no. 2, p. 90, Feb. 1989.
[10] R. A. Chipman, "Order dependence and independence of weak polarization elements," *Proc. SPIE*, vol. 1166, pp. 135–142, Jan. 1990.
[11] H. D. Shi, H. L. Jiang, and X. Zhang, "Research on freeform optical system aberration characteristic based on vector aberration," *Acta Optica Sinica*, vol. 35, no. 12, p. 118, 2015.
[12] H. D. Shi, X. Zhang, and Y. C. Li, "Analysis of aberration properties of pupil off-axis freeform surface optical system," *Acta Optica Sinica*, vol. 429, no. 12, p. 94, 2015.
[13] J. Luo, X. He, and K. Fan, "Polarization aberrations in an unobscures off-axis astronomical telescope and their effects on optics ellipticity," *Acta Optica Sinica*, vol. 461, no. 8, p. 55, 2020.
[14] R. A. Chipman, "Mechanics of polarization ray tracing," *Opt. Eng.*, vol. 34, no. 6, p. 1636, Jun. 1995.
[15] M. Shribak, "Polarization aberrations caused by differential transmission and phase shift in high-numerical-aperture lenses: Theory, measurement, and rectification," *Opt. Eng.*, vol. 41, no. 5, p. 943, May 2002.
[16] R. A. Chipman and L. J. Chipman, "Polarization aberration diagrams," *Opt. Eng.*, vol. 28, no. 2, p. 100, Feb. 1989.
[17] M. Totzeck, P. Graupner, and T. Heil, "How to describe polarization influence on imaging," *Proc. SPIE*, vol. 5754, pp. 23–37, May 2004.
[18] Y. B. Liao, *Polarization Optics*. Beijing, China: Science Press, 2003, pp. 45–63.
[19] G. Yun, K. Crabtree, and R. A. Chipman, "Three-dimensional polarization ray-tracing calculus I: Definition and diattenuation," *Appl. Opt.*, vol. 50, no. 18, p. 2855, Jun. 2011.
[20] G. Yun, S. C. McClain, and R. A. Chipman, "Three-dimensional polarization ray-tracing calculus II: Retardance," *Appl. Opt.*, vol. 50, no. 18, p. 2866, Jun. 2011.
[21] Q. T. Liang, *Physical Optics*. Beijing, China: Publishing House of Electronics Industry, 2012, pp. 36–38.

YILAN ZHANG was born in Jilin, China, in 1992. She received the bachelor's and master's degrees in optoelectronic information engineering from the Changchun University of Science and Technology, in 2015 and 2018, respectively, where she is currently pursuing the Ph.D. degree.

She has published three academic articles in journals included in domestic EI such as "*Optics Acta*." Her research interests include polarization aberration research and optical design.

HAODONG SHI was born in Jilin, China, in 1989. He received the Ph.D. degree in optical engineering from the Changchun University of Science and Technology, in 2017.

Since 2017, he has been a Lecturer with the Changchun University of Science and Technology. He has published 13 academic articles in journals included in SCI and EI at home and abroad, such as *Applied Optics* and *Optica Acta*. His research interests include optical system design, free-form surface optical system aberration theory, polarization detection, and calibration technology. He successively undertook six national scientific research projects, such as the National Natural Science Foundation of China, the Astronomical Joint Fund, the Youth Fund, the National Key Research and Development Program, the National Civil Aerospace, and the Military Commission Science and Technology Commission, and three provincial and ministerial scientific research projects.

HUILIN JIANG was born in Liaozhong, Liaoning, China, in 1945. He graduated from the Changchun Institute of Optics and Mechanics, in 1969, and from the Changchun Institute of Optics and Mechanics, Chinese Academy of Sciences, in 1987.

He used to be the President of the Changchun University of Science and Technology, where he is currently the Director of the Academic Committee of the school.

Dr. Jiang concurrently serves as the Vice Chairperson of the Chinese Ordnance Society, the Standing Director of the Chinese Optical Society and the Chinese Optical Engineering Society, a member of the Expert Committee of the Aerospace Field of the Central Military Commission Science and Technology Commission, and the Deputy Director of the Academic Committee of the State Key Laboratory of Applied Optics, Changchun Institute of Optics and Mechanics. He was elected as an Academician of the Chinese Academy of Engineering, in 2015. He has engaged in the research of applied optics technology for a long time, and has presided over 36 national "863" key projects and the National Natural Science Foundation of China. He won the third prize and second prize from the National Science and Technology Progress Award, in 1996 and 2009, respectively. In 2010, he also won the second prize from the National Technology Invention. In 2014, he won the He Liang He Li Fund Science and Technology Progress Award for the fundamental study of plasma sources, and fabrication of micro or nanostructured surfaces.